



1
2
3
4
5
6
7
8
9
10
11
12
13
14
15
16
17
18
19
20
21
22
23
24
25
26
27
28
29
30
31
32
33
34
35
36
37
38
39
40
41
42
43
44
45
46
47
48

Mitochondrial respiratory states and rates

COST Action CA15203 MitoEAGLE preprint Version: 2018-11-30 (48)

Corresponding author: Gnaiger E

Authors:

Gnaiger E, Aasander Frostner E, Abumrad NA, Acuna-Castroviejo D, Ahn B, Ali SS, Alton L, Alves MG, Amati F, Amoedo ND, Andreadou I, Arago Belenguer M, Aral C, Arandarčikaitė O, Armand AS, Arnould T, Avram VF, Bailey DM, Bajpeyi S, Bajzikova M, Bakker BM, Bastos Sant'Anna Silva AC, Batterson P, Battino M, Bazil J, Beard DA, Bednarczyk P, Bello F, Ben-Shachar D, Bergdahl A, Berge RK, Bergmeister L, Bernardi P, Berridge MV, Bettinazzi S, Bishop D, Blier PU, Blindheim DF, Boardman NT, Boetker HE, Borchard S, Boros M, Børsheim E, Borutaite V, Botella Ruiz J, Bouillaud F, Bouitbir J, Boushel RC, Bovard J, Breton S, Brown DA, Brown GC, Brown RA, Brozinick JT, Buettner GR, Burtscher J, Calabria E, Calbet JA, Calzia E, Cannon DT, Cano Sanchez M, Canto AC, Cardoso LHD, Carvalho E, Casado Pinna M, Cassar S, Cassina AM, Castelo MP, Castro L, Cavalcanti-de-Albuquerque JP, Cervinkova Z, Chabi B, Chakrabarti L, Chaurasia B, Chen Q, Chicco AJ, Chinopoulos C, Chowdhury SK, Cizmarova B, Clementi E, Coen PM, Cohen BH, Coker RH, Collin A, Crisóstomo L, Dahdah N, Dambrova M, Danhelovska T, Darveau CA, Das AM, Dash RK, Davidova E, Davis MS, De Goede P, De Palma C, Dembinska-Kiec A, Detraux D, Devaux Y, Di Marcello M, Dias TR, Distefano G, Doermann N, Doerrier C, Dong L, Donnelly C, Drahota Z, Dubouchaud H, Duchon MR, Dumas JF, Durham WJ, Dymkowska D, Dyrstad SE, Dyson A, Dzialowski EM, Ehinger J, Elmer E, Endlicher R, Engin AB, Escames G, Ezrova Z, Falk MJ, Fell DA, Ferdinandy P, Ferko M, Ferreira JCB, Ferreira R, Ferri A, Fessel JP, Filipovska A, Fisar Z, Fischer C, Fischer M, Fisher G, Fisher JJ, Ford E, Fornaro M, Galina A, Galkin A, Galli GL, Gan Z, Ganetzky R, Garcia-Roves PM, Garcia-Souza LF, Garipi E, Garlid KD, Garrabou G, Garten A, Gastaldelli A, Gayen J, Genders A, Genova ML, Giovarelli M, Gonzalez-Armenta JL, Goncalo Teixeira da SR, Gonzalo H, Goodpaster BH, Gorr TA, Gourlay CW, Granata C, Grefte S, Guarch ME, Gueguen N, Gumeni S, Haas CB, Haavik J, Haendeler J, Hamann A, Han J, Han WH, Hancock CR, Hand SC, Handl J, Hargreaves IP, Harper ME, Harrison DK, Hausenloy DJ, Heales SJR, Heiestad C, Hellgren KT, Hepple RT, Hernansanz-Agustin P, Hewakapuge S, Hickey AJ, Hoel F, Holland OJ, Holloway GP, Hoppel CL, Hoppel F, Houstek J, Huete-Ortega M, Hyrossova P, Iglesias-Gonzalez J, Irving BA, Isola R, Iyer S, Jackson CB, Jadiya P, Jang DH, Jang YC, Janowska J, Jansen K, Jansen-Dürr P, Jansone B, Jarmuszkiewicz W, Jaskiewicz A, Jespersen NR, Jha RK, Jurczak MJ, Jurk D, Kaambre T, Kaczor JJ, Kainulainen H, Kampa RP, Kandel SM, Kane DA, Kang Y, Kappler L, Karabatsiakakis A, Karkucinska-Wieckowska A, Kaur S, Keijer J, Keller MA, Keppner G, Khamoui AV, Kidere D, Kilbaugh T, Kim HK, Kim JKS, Klepinin A, Klingenspor M, Komlodi T, Koopman WJH, Kopitar-Jerala N, Kowaltowski AJ, Kozlov AV, Krajcova A, Krako Jakovljevic N, Kristal BS, Krycer JR, Kuang J, Kucera O, Kuka J, Kwak HB, Kwast K, Laasmaa M, Labieniec-Watala M, Lai N, Land JM, Lane N, Laner V, Lanza IR, Larsen TS, Lavery GG, Lazou A, Lee HK, Leeuwenburgh C, Lehti M, Lemieux H, Lenaz G, Lerfall J, Li PA, Li Puma L, Liepins E, Lionett S, Liu J, López LC, Lucchinetti E, Ma T, Macedo MP, MacMillan-Crow LA, Majtnerova P, Makarova E, Makrecka-Kuka M, Malik AN, Markova M, Martins AD, Martin DS, Martins JD, Mazat JP, McKenna HT, Menze MA, Merz T, Meszaros AT, Methner A, Michalak S, Moellering DR, Moiso N, Molina AJA, Montaigne D, Moore AL, Moreau K, Moreno-Sánchez R, Moreira BP, Mracek T, Muccini AM, Muntane J, Muntean DM, Murray AJ, Musiol E, Myhre Pedersen T, Nair KS, Nehlin JO, Nemeč M, Neuffer PD, Neuzil J, Nevriere R, Newsom S, Nozickova K, O'Brien KA, O'Gorman D, Olgar

49 Y, Oliveira MF, Oliveira MT, Oliveira PF, Oliveira PJ, Orynbayeva Z, Osiewacz HD, Ounpuu L, Pak
 50 YK, Pallotta ML, Palmeira CM, Parajuli N, Passos JF, Passrigger M, Patel HH, Pavlova N, Pecina P,
 51 Pereira da Silva Grilo da Silva F, Perez Valencia JA, Perks K, Pesta D, Petit PX, Pettersen IKN, Pichaud
 52 N, Pichler I, Piel S, Pietka TA, Pino MF, Pirkmajer S, Porter C, Porter RK, Pranger F, Prochownik EV,
 53 Pulinilkunnil T, Puskarich MA, Puurand M, Quijano C, Radenkovic F, Radi R, Ramzan R, Rattan SIS,
 54 Reboredo P, Renner-Sattler K, Rial E, Robinson MM, Roden M, Rodríguez-Enriquez S, Rohlena J, Rolo
 55 AP, Ropelle ER, Røslund GV, Rossignol R, Rossiter HB, Rubelj I, Rybacka-Mossakowska J, Saada A,
 56 Safaei Z, Salin K, Salvadego D, Sandi C, Saner N, Sanz A, Sazanov LA, Scatena R, Schartner M,
 57 Scheibye-Knudsen M, Schilling JM, Schlattner U, Schönfeld P, Schots PC, Schulz R, Schwarzer C,
 58 Scott GR, Selman C, Shabalina IG, Sharma P, Sharma V, Shevchuk I, Siewiera K, Silber AM, Silva
 59 AM, Sims CA, Singer D, Skolik R, Smenes BT, Smith J, Soares FAA, Sobotka O, Sokolova I, Sonkar
 60 VK, Sowton AP, Sparagna GC, Sparks LM, Spinazzi M, Stankova P, Starr J, Stary C, Stelfa G, Stepto
 61 NK, Stiban J, Stier A, Stocker R, Storder J, Sumbalova Z, Suravajhala P, Svalbe B, Swerdlow RH,
 62 Swiniuch D, Szabo I, Szewczyk A, Szibor M, Tanaka M, Tandler B, Tarnopolsky MA, Tausan D,
 63 Tavernarakis N, Tepp K, Thakkar H, Thyfault JP, Tomar D, Torp MK, Towheed A, Tretter L, Trifunovic
 64 A, Trivigno C, Tronstad KJ, Trougakos IP, Truu L, Tuncay E, Turan B, Tyrrell DJ, Urban T, Valentine
 65 JM, Vella J, Vendelin M, Vercesi AE, Victor VM, Vieira Ligo Teixeira C, Vidimce J, Viel C, Vieyra
 66 A, Vilks K, Villena JA, Vincent V, Vinogradov AD, Viscomi C, Vitorino RMP, Vogt S, Volani C,
 67 Volska K, Votion DM, Vujacic-Mirski K, Wagner BA, Ward ML, Warnsmann V, Wasserman DH,
 68 Watala C, Wei YH, Whitfield J, Wickert A, Wieckowski MR, Wiesner RJ, Williams C, Winwood-Smith
 69 H, Wohlgemuth SE, Wohlwend M, Wolff JN, Wrutniak-Cabello C, Wüst RCI, Yokota T, Zablocki K,
 70 Zanon A, Zaugg K, Zaugg M, Zdrzilova L, Zhang Y, Zhang YZ, Ziková A, Zischka H, Zorzano A,
 71 Zvejniece L

72

73

Updates and discussion:

74

http://www.mitoeagle.org/index.php/MitoEAGLE_preprint_2018-02-08

75

76

491 co-authors

77

78

Correspondence: Gnaiger E

79

Chair COST Action CA15203 MitoEAGLE – <http://www.mitoeagle.org>

80

Department of Visceral, Transplant and Thoracic Surgery, D. Swarovski Research Laboratory,

81

Medical University of Innsbruck, Innrain 66/4, A-6020 Innsbruck, Austria

82

Email: mitoeagle@i-med.ac.at; Tel: +43 512 566796, Fax: +43 512 566796 20

83



84	Table of contents
85	
86	Abstract
87	Executive summary
88	1. Introduction – Box 1: In brief: Mitochondria and Bioblasts
89	2. Coupling states and rates in mitochondrial preparations
90	2.1. <i>Cellular and mitochondrial respiration</i>
91	2.1.1. Aerobic and anaerobic catabolism and ATP turnover
92	2.1.2. Specification of biochemical dose
93	2.2. <i>Mitochondrial preparations</i>
94	2.3. <i>Electron transfer pathways</i>
95	2.4. <i>Respiratory coupling control</i>
96	2.4.1. Coupling
97	2.4.2. Phosphorylation, P_{\gg} , and P_{\gg}/O_2 ratio
98	2.4.3. Uncoupling
99	2.5. <i>Coupling states and respiratory rates</i>
100	2.5.1. LEAK-state
101	2.5.2. OXPHOS-state
102	2.5.3. Electron transfer-state
103	2.5.4. ROX state and <i>Rox</i>
104	2.5.5. Quantitative relations
105	2.5.6. The steady-state
106	2.6. <i>Classical terminology for isolated mitochondria</i>
107	2.6.1. State 1
108	2.6.2. State 2
109	2.6.3. State 3
110	2.6.4. State 4
111	2.6.5. State 5
112	2.7. <i>Control and regulation</i>
113	3. What is a rate? – Box 2: Metabolic flows and fluxes: vectorial, vectorial, and scalar
114	4. Normalization of rate per sample
115	4.1. <i>Flow: per object</i>
116	4.1.1. Number concentration
117	4.1.2. Flow per object
118	4.2. <i>Size-specific flux: per sample size</i>
119	4.2.1. Sample concentration
120	4.2.2. Size-specific flux
121	4.3. <i>Marker-specific flux: per mitochondrial content</i>
122	4.3.1. Mitochondrial concentration and mitochondrial markers
123	4.3.2. mt-Marker-specific flux
124	5. Normalization of rate per system
125	5.1. <i>Flow: per chamber</i>
126	5.2. <i>Flux: per chamber volume</i>
127	5.2.1. System-specific flux
128	5.2.2. Advancement per volume
129	6. Conversion of units
130	7. Conclusions – Box 3: Recommendations for studies with mitochondrial preparations
131	References
132	Supplement
133	S1. Manuscript phases and versions - an open-access approach
134	S2. Authors
135	S3. Joining COST Actions
136	

137 **Abstract** As the knowledge base and importance of mitochondrial physiology to human health expands,
 138 the necessity for harmonizing the terminology concerning mitochondrial respiratory states and rates has
 139 become increasingly apparent. The chemiosmotic theory establishes the mechanism of energy
 140 transformation and coupling in oxidative phosphorylation. The unifying concept of the protonmotive
 141 force provides the framework for developing a consistent theoretical foundation of mitochondrial
 142 physiology and bioenergetics. We follow IUPAC guidelines on terminology in physical chemistry,
 143 extended by considerations of open systems and thermodynamics of irreversible processes. The concept-
 144 driven constructive terminology incorporates the meaning of each quantity and aligns concepts and
 145 symbols with the nomenclature of classical bioenergetics. We endeavour to provide a balanced view of
 146 mitochondrial respiratory control and a critical discussion on reporting data of mitochondrial respiration
 147 in terms of metabolic flows and fluxes. Uniform standards for evaluation of respiratory states and rates
 148 will ultimately contribute to reproducibility between laboratories and thus support the development of
 149 databases of mitochondrial respiratory function in species, tissues, and cells. Clarity of concept and
 150 consistency of nomenclature facilitate effective transdisciplinary communication, education, and
 151 ultimately further discovery.

152
 153 *Keywords:* Mitochondrial respiratory control, coupling control, mitochondrial preparations,
 154 protonmotive force, uncoupling, oxidative phosphorylation: OXPHOS, efficiency, electron transfer: ET,
 155 electron transfer system: ETS, proton leak, ion leak and slip compensatory state: LEAK, residual oxygen
 156 consumption: ROX, State 2, State 3, State 4, normalization, flow, flux, oxygen: O₂
 157

158 **Executive summary**

159
 160 In view of the broad implications for health care, mitochondrial researchers face an increasing
 161 responsibility to disseminate their fundamental knowledge and novel discoveries to a wide range of
 162 stakeholders and scientists beyond the group of specialists. This requires implementation of a commonly
 163 accepted terminology within the discipline and standardization in the translational context. Authors,
 164 reviewers, journal editors, and lecturers are challenged to collaborate with the aim to harmonize the
 165 nomenclature in the growing field of mitochondrial physiology and bioenergetics, from evolutionary
 166 biology and comparative physiology to mitochondrial medicine. In the present communication we focus
 167 on the following concepts in mitochondrial physiology:

- 168 1. Aerobic respiration depends on the coupling of phosphorylation (ADP → ATP) to O₂ flux in
 169 catabolic reactions. Coupling in oxidative phosphorylation is mediated by the translocation of
 170 protons across the mitochondrial inner membrane (mtIM) through proton pumps generating
 171 or utilizing the protonmotive force that is maintained between the mitochondrial matrix and
 172 intermembrane compartment or outer mitochondrial space. Compartmental coupling
 173 distinguishes this vectorial component of oxidative phosphorylation from glycolytic
 174 fermentation as the counterpart of cellular core energy metabolism (**Figure 1**). Cell respiration
 175 is distinguished from fermentation: (1) Electron acceptors are supplied by external respiration
 176 for the maintenance of redox balance, whereas fermentation is characterized by an internal
 177 electron acceptor produced in intermediary metabolism. In aerobic cell respiration, redox
 178 balance is maintained by O₂ as the electron acceptor. (2) Compartmental coupling in vectorial
 179 oxidative phosphorylation contrasts to exclusively scalar substrate-level phosphorylation in
 180 fermentation.
- 181 2. When measuring mitochondrial metabolism, the contribution of fermentation and other cytosolic
 182 interactions must be excluded from analysis by disrupting the barrier function of the plasma
 183 membrane. Selective removal or permeabilization of the plasma membrane yields
 184 mitochondrial preparations—including isolated mitochondria, tissue and cellular
 185 preparations—with structural and functional integrity. Subsequently, extra-mitochondrial
 186 concentrations of fuel substrates, ADP, ATP, inorganic phosphate, and cations including H⁺
 187 can be controlled to determine mitochondrial function under a set of conditions defined as
 188 coupling control states. We strive to incorporate an easily recognized and understood concept-
 189 driven terminology of bioenergetics with explicit terms and symbols that define the nature of
 190 respiratory states.
- 191 3. Mitochondrial coupling states are defined according to the control of respiratory oxygen flux by
 192 the protonmotive force. Capacities of oxidative phosphorylation and electron transfer are

measured at kinetically saturating concentrations of fuel substrates, ADP and inorganic phosphate, and O₂, or at optimal uncoupler concentrations, respectively, in the absence of Complex IV inhibitors such as NO, CO, or H₂S. Respiratory capacity is a measure of the upper boundary of the rate of respiration; it depends on the substrate type undergoing oxidation, and provides reference values for the diagnosis of health and disease, and for evaluation of the effects of Evolutionary background, Age, Gender and sex, Lifestyle and Environment.

Figure 1. Internal and external respiration

Mitochondrial respiration is the oxidation of fuel substrates (electron donors) and reduction of O₂ catalysed by the electron transfer system, ETS: (mt) mitochondrial catabolic respiration; (ce) total cellular O₂ consumption; and (ext) external respiration. All chemical reactions, r , that consume O₂ in the cells of an organism, contribute to cell respiration, J_{rO_2} . In addition to mitochondrial catabolic respiration, O₂ is consumed by:

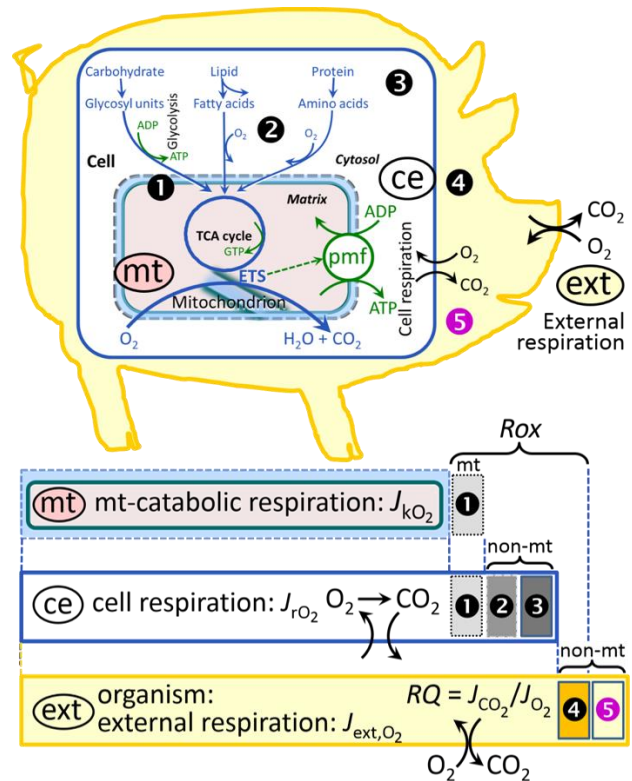
① Mitochondrial residual O₂ consumption, Rox .
 ② Non-mitochondrial O₂ consumption by catabolic reactions, particularly peroxisomal oxidases and microsomal cytochrome P450 systems. ③ Non-mitochondrial Rox by reactions unrelated to catabolism. ④ Extracellular Rox . ⑤ Aerobic microbial respiration. Bars are not at a quantitative scale.

(mt) **Mitochondrial catabolic respiration**, J_{kO_2} , is the O₂ consumption by the mitochondrial ETS excluding Rox .

(ce) **Cell respiration**, J_{rO_2} , takes into account

internal O₂-consuming reactions, r , including catabolic respiration and Rox . Catabolic cell respiration is the O₂ consumption associated with catabolic pathways in the cell, including mitochondrial catabolism in addition to peroxisomal and microsomal oxidation reactions (②).

(ext) **External respiration** balances internal respiration at steady-state, including extracellular Rox (④) and aerobic respiration by the microbiome (⑤). O₂ is transported from the environment across the respiratory cascade, *i.e.*, circulation between tissues and diffusion across cell membranes, to the intracellular compartment. The respiratory quotient, RQ , is the molar CO₂/O₂ exchange ratio; when combined with the respiratory nitrogen quotient, N/O₂ (mol N given off per mol O₂ consumed), the RQ reflects the proportion of carbohydrate, lipid and protein utilized in cell respiration during aerobically balanced steady-states. Bicarbonate and CO₂ are transported in reverse to the extracellular milieu and the organismic environment. Hemoglobin provides the molecular paradigm for the combination of O₂ and CO₂ exchange, as do lungs and gills on the morphological level.



4. Incomplete tightness of coupling, *i.e.*, some degree of uncoupling relative to the substrate-dependent coupling stoichiometry, is a characteristic of energy-transformations across membranes. Uncoupling is caused by a variety of physiological, pathological, toxicological, pharmacological and environmental conditions that exert an influence not only on the proton leak and cation cycling, but also on proton slip within the proton pumps and the structural integrity of the mitochondria. A more loosely coupled state is induced by stimulation of mitochondrial superoxide formation and the bypass of proton pumps. In addition, the use of protonophores represents an experimental uncoupling intervention to assess the transition from a well-coupled to a noncoupled state of mitochondrial respiration.

5. Respiratory oxygen consumption rates have to be carefully normalized to enable meta-analytic studies beyond the question of a particular experiment. Therefore, all raw data on rates and variables for normalization should be published in an open access data repository. Normalization of rates for: (1) the number of objects (cells, organisms); (2) the volume or

mass of the experimental sample; and (3) the concentration of mitochondrial markers in the experimental chamber are sample-specific normalizations, which are distinguished from system-specific normalization for the volume of the chamber (the measuring system).

6. The consistent use of terms and symbols will facilitate transdisciplinary communication and support the further development of a collaborative database on bioenergetics and mitochondrial physiology. The present considerations are focused on studies with mitochondrial preparations. These will be extended in a series of reports on pathway control of mitochondrial respiration, respiratory states in intact cells, and harmonization of experimental procedures.

Box 1: In brief – Mitochondria and Bioblasts

‘For the physiologist, mitochondria afforded the first opportunity for an experimental approach to structure-function relationships, in particular those involved in active transport, vectorial metabolism, and metabolic control mechanisms on a subcellular level’ (Ernster and Schatz 1981).

Mitochondria are oxygen-consuming electrochemical generators that evolved from the endosymbiotic alphaproteobacteria which became integrated into a host cell related to Asgard Archaea (Margulis 1970; Lane 2005; Roger *et al.* 2017). They were described by Richard Altmann (1894) as ‘bioblasts’, which include not only the mitochondria as presently defined, but also symbiotic and free-living bacteria. The word ‘mitochondria’ (Greek mitos: thread; chondros: granule) was introduced by Carl Benda (1898).

Contrary to current textbook dogma, mitochondria form dynamic networks within eukaryotic cells. Mitochondrial movement is supported by microtubules and morphology can change in response to energy requirements of the cell via processes known as fusion and fission; these interactions allow mitochondria to communicate within a network (Chan 2006). Mitochondria can even traverse cell boundaries in a process known as horizontal mitochondrial transfer (Torralba *et al.* 2016). Another defining characteristic of mitochondria is the double membrane. The mitochondrial inner membrane (mtIM) forms dynamic tubular to disk-shaped cristae that separate the mitochondrial matrix, *i.e.*, the negatively charged internal mitochondrial compartment, from the intermembrane space; the latter being enclosed by the mitochondrial outer membrane (mtOM) and positively charged with respect to the matrix. The mtIM contains the non-bilayer phospholipid cardiolipin, which is not present in any other eukaryotic cellular membrane. Cardiolipin has many regulatory functions (Oemer *et al.* 2018); in particular, it stabilizes and promotes the formation of respiratory supercomplexes (SC I_nIII_nIV_n), which are supramolecular assemblies based upon specific and dynamic interactions between individual respiratory complexes (Greggio *et al.* 2017; Lenaz *et al.* 2017). The mitochondrial membrane is plastic and exerts an influence on the functional properties of proteins incorporated in membranes (Waczulikova *et al.* 2007). Intracellular stress factors may cause shrinking or swelling of the mitochondrial matrix that can ultimately result in permeability transition.

Mitochondria are the structural and functional elementary components of cell respiration. Mitochondrial respiration is the reduction of molecular oxygen by electron transfer coupled to electrochemical proton translocation across the mtIM. In the process of oxidative phosphorylation (OXPHOS), the catabolic reaction of oxygen consumption is electrochemically coupled to the transformation of energy in the form of adenosine triphosphate (ATP; Mitchell 1961, 2011). Mitochondria are the powerhouses of the cell that contain the machinery of the OXPHOS-pathways, including transmembrane respiratory complexes (proton pumps with FMN, Fe-S and cytochrome *b*, *c*, *aa*₃ redox systems); alternative dehydrogenases and oxidases; the coenzyme ubiquinone (Q); F-ATPase or ATP synthase; the enzymes of the tricarboxylic acid cycle (TCA), fatty acid and amino acid oxidation; transporters of ions, metabolites and co-factors; iron/sulphur cluster synthesis; and mitochondrial kinases related to catabolic pathways. The mitochondrial proteome comprises over 1,200 proteins (Calvo *et al.* 2015; 2017), mostly encoded by nuclear DNA (nDNA), with a variety of functions, many of which are relatively well known, *e.g.*, proteins regulating mitochondrial biogenesis or apoptosis, while others are still under investigation, or need to be identified, *e.g.*, permeability transition pore, alanine transporter. Only recently has it been possible to use the mammalian mitochondrial proteome to discover and characterize the genetic basis of mitochondrial diseases (Williams *et al.* 2016; Palmfeldt and Bross 2017).

Numerous cellular processes are orchestrated by a constant crosstalk between mitochondria and other cellular components. For example, the crosstalk between mitochondria and the endoplasmic

reticulum is involved in the regulation of calcium homeostasis, cell division, autophagy, differentiation, and anti-viral signaling (Murley and Nunnari 2016). Mitochondria contribute to the formation of peroxisomes, which are hybrids of mitochondrial and ER-derived precursors (Sugiura *et al.* 2017). Cellular mitochondrial homeostasis (mitostasis) is maintained through regulation at transcriptional, post-translational and epigenetic levels. Cell signalling modules contribute to homeostatic regulation throughout the cell cycle or even cell death by activating proteostatic modules, *e.g.*, the ubiquitin-proteasome and autophagy-lysosome/vacuole pathways; specific proteases like LON, and genome stability modules in response to varying energy demands and stress cues (Quiros *et al.* 2016). Several post-translational modifications, including acetylation and nitrosylation, are also capable of influencing the bioenergetic response, with clinically significant implications for health and disease (Carrico *et al.* 2018).

Mitochondria of higher eukaryotes typically maintain several copies of their own circular genome known as mitochondrial DNA (mtDNA; hundred to thousands per cell; Cummins 1998), which is maternally inherited in humans. Biparental mitochondrial inheritance is documented in mammals, birds, fish, reptiles and invertebrate groups, and is even the norm in some bivalve taxonomic groups (Breton *et al.* 2007; White *et al.* 2008). The mitochondrial genome of the angiosperm *Amborella* contains a record of six mitochondrial genome equivalents acquired by horizontal transfer of entire genomes, two from angiosperms, three from algae and one from mosses (Rice *et al.* 2016). In unicellular organisms, *i.e.*, protists, the structural organization of mitochondrial genomes is highly variable and includes circular and linear DNA (Zikova *et al.* 2016). While some of the free-living flagellates exhibit the largest known gene coding capacity, *e.g.*, jakobid *Andalucia godoyi* mitochondrial DNA codes for 106 genes (Burger *et al.* 2013), some protist groups, *e.g.*, alveolates, possess mitochondrial genomes with only three protein-coding genes and two rRNAs (Feagin *et al.* 2012). The complete loss of mitochondrial genome is observed in highly reduced mitochondria of *Cryptosporidium* species (Liu *et al.* 2016). Reaching the final extreme, the microbial eukaryote, oxymonad *Monocercomonoides*, has no mitochondrion whatsoever and lacks all typical nuclear-encoded mitochondrial proteins, showing that while in 99% of organisms mitochondria play a vital role, this organelle is not indispensable (Karnkowska *et al.* 2016).

In vertebrates but not all invertebrates, mtDNA is compact (16.5 kB in humans) and encodes 13 protein subunits of the transmembrane respiratory Complexes CI, CIII, CIV and ATP synthase (F-ATPase), 22 tRNAs, and two rRNAs. Additional gene content has been suggested to include microRNAs, piRNA, smithRNAs, repeat associated RNA, and even additional proteins (Duarte *et al.* 2014; Lee *et al.* 2015; Cobb *et al.* 2016). The mitochondrial genome requires nuclear-encoded mitochondrially targeted proteins, *e.g.*, TFAM, for its maintenance and expression (Rackham *et al.* 2012). Both genomes encode peptides of the membrane spanning redox pumps (CI, CIII and CIV) and F-ATPase, leading to strong constraints in the coevolution of both genomes (Blier *et al.* 2001).

Given the multiple roles of mitochondria, it is perhaps not surprising that mitochondrial dysfunction is associated with a wide variety of genetic and degenerative diseases. Robust mitochondrial function is supported by physical exercise and caloric balance, and is central for sustained metabolic health throughout life. Therefore, a more consistent set of definitions for mitochondrial physiology will increase our understanding of the etiology of disease and improve the diagnostic repertoire of mitochondrial medicine with a focus on protective medicine, lifestyle and healthy aging.

Mitochondrion is singular and mitochondria is plural. Abbreviation: mt, as generally used in mtDNA.

1. Introduction

Mitochondria are the powerhouses of the cell with numerous physiological, molecular, and genetic functions (**Box 1**). Every study of mitochondrial health and disease faces **Evolution, Age, Gender and sex, Lifestyle, and Environment (MitoEAGLE)** as essential background conditions intrinsic to the individual person or cohort, species, tissue and to some extent even cell line. As a large and coordinated group of laboratories and researchers, the mission of the global MitoEAGLE Network is to generate the necessary scale, type, and quality of consistent data sets and conditions to address this intrinsic complexity. Harmonization of experimental protocols and implementation of a quality control

361 and data management system are required to interrelate results gathered across a spectrum of studies
362 and to generate a rigorously monitored database focused on mitochondrial respiratory function. In this
363 way, researchers from a variety of disciplines can compare their findings using clearly defined and
364 accepted international standards.

365 With an emphasis on quality of research, published data can be useful far beyond the specific
366 question of a particular experiment. For example, collaborative data sets support the development of
367 open-access databases such as those for National Institutes of Health sponsored research in genetics,
368 proteomics, and metabolomics. Indeed, enabling meta-analysis is the most economic way of providing
369 robust answers to biological questions (Cooper *et al.* 2009). However, the reproducibility of quantitative
370 results and databases depend on accurate measurements under strictly-defined conditions. Likewise,
371 meaningful interpretation and comparability of experimental outcomes requires standardisation of
372 protocols between research groups at different institutes. In addition to quality control, a conceptual
373 framework is also required to standardise and homogenise terminology and methodology. Vague or
374 ambiguous jargon can lead to confusion and may convert valuable signals to wasteful noise. For this
375 reason, measured values must be expressed in standard units for each parameter used to define
376 mitochondrial respiratory function. A consensus on fundamental nomenclature and conceptual
377 coherence, however, are missing in the expanding field of mitochondrial physiology. To fill this gap,
378 the present communication provides an in-depth review on harmonization of nomenclature and
379 definition of technical terms, which are essential to improve the awareness of the intricate meaning of
380 current and past scientific vocabulary. This is important for documentation and integration into
381 databases in general, and quantitative modelling in particular (Beard 2005).

382 In this review, we focus on coupling states and fluxes through metabolic pathways of aerobic
383 energy transformation in mitochondrial preparations as a first step in the attempt to generate a
384 conceptually-oriented nomenclature in bioenergetics and mitochondrial physiology. Respiratory control
385 by fuel substrates and specific inhibitors of respiratory enzymes, coupling states of intact cells, and
386 respiratory flux control ratios will be reviewed in subsequent communications, prepared in the frame of
387 COST Action MitoEAGLE open to global bottom-up input.

388
389

390 **2. Coupling states and rates in mitochondrial preparations**

391 *‘Every professional group develops its own technical jargon for talking about matters of critical*
392 *concern ... People who know a word can share that idea with other members of their group, and*
393 *a shared vocabulary is part of the glue that holds people together and allows them to create a*
394 *shared culture’* (Miller 1991).

395

396 *2.1. Cellular and mitochondrial respiration*

397

398 **2.1.1. Aerobic and anaerobic catabolism and ATP turnover:** In respiration, electron transfer
399 is coupled to the phosphorylation of ADP to ATP, with energy transformation mediated by the
400 protonmotive force, pmf (**Figure 2**). Anabolic reactions are coupled to catabolism, both by ATP as the
401 intermediary energy currency and by small organic precursor molecules as building blocks for
402 biosynthesis. Glycolysis involves substrate-level phosphorylation of ADP to ATP in fermentation
403 without utilization of O₂, studied mainly in intact cells and organisms. Many cellular fuel substrates are
404 catabolized to acetyl-CoA or to glutamate, and further electron transfer reduces nicotinamide adenine
405 dinucleotide to NADH or flavin adenine dinucleotide to FADH₂. Subsequent mitochondrial electron
406 transfer to O₂ is coupled to proton translocation for the control of the protonmotive force and
407 phosphorylation of ADP (**Figure 2B and 2C**). In contrast, extra-mitochondrial oxidation of fatty acids
408 and amino acids proceeds partially in peroxisomes without coupling to ATP production: acyl-CoA
409 oxidase catalyzes the oxidation of FADH₂ with electron transfer to O₂; amino acid oxidases oxidize
410 flavin mononucleotide FMNH₂ or FADH₂ (**Figure 2A**).

411

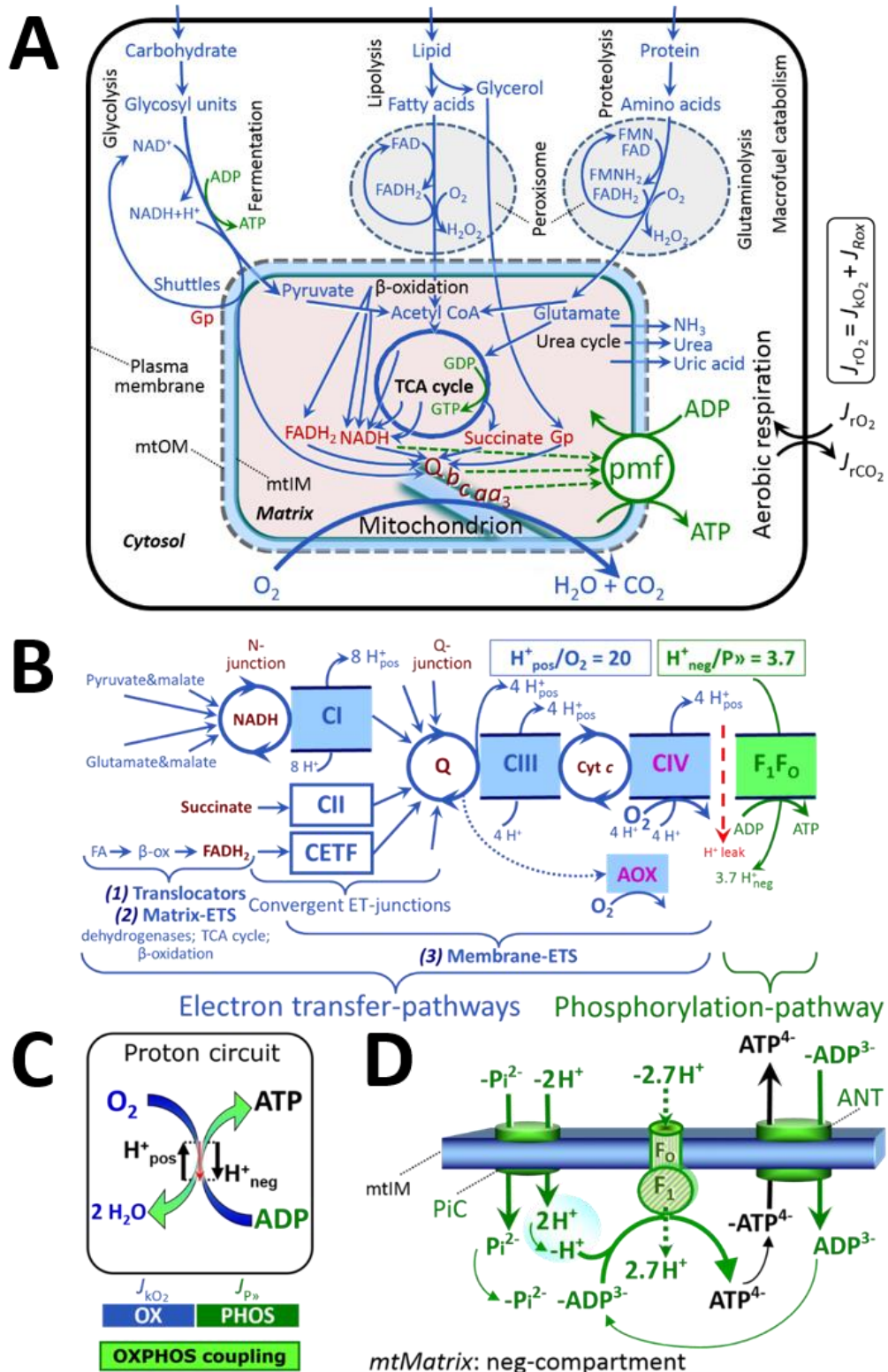


Figure 2. Cell respiration and oxidative phosphorylation (OXPHOS)

Mitochondrial respiration is the oxidation of fuel substrates (electron donors) with electron transfer to O_2 as the electron acceptor. For explanation of symbols see also **Figure 1**.

(A) Respiration of intact cells: Extra-mitochondrial catabolism of macrofuels and uptake of small molecules by the cell provide the mitochondrial fuel substrates. Dashed arrows indicate the connection between the redox proton pumps (respiratory Complexes CI, CIII and CIV) and the transmembrane protonmotive force, pmf. Coenzyme Q (Q) and the cytochromes *b*, *c*, and *aa₃* are redox systems of the mitochondrial inner membrane, mtIM. Glycerol-3-phosphate, Gp.

412
413
414
415
416
417
418
419
420
421

422 (B) Respiration in mitochondrial preparations: The mitochondrial electron transfer system
 423 (ETS) is (1) fuelled by diffusion and transport of substrates across the mtOM and mtIM,
 424 and in addition consists of the (2) matrix-ETS, and (3) membrane-ETS. Electron transfer
 425 converges at the N-junction, and from CI, CII and electron transferring flavoprotein
 426 complex (CETF) at the Q-junction. Unlabeled arrows converging at the Q-junction indicate
 427 additional ETS-sections with electron entry into Q through glycerophosphate
 428 dehydrogenase, dihydro-orotate dehydrogenase, proline dehydrogenase, choline
 429 dehydrogenase, and sulfide-ubiquinone oxidoreductase. The dotted arrow indicates the
 430 branched pathway of oxygen consumption by alternative quinol oxidase (AOX). ET-
 431 pathways are coupled to the phosphorylation-pathway. The H^+_{pos}/O_2 ratio is the outward
 432 proton flux from the matrix space to the positively (pos) charged vesicular compartment,
 433 divided by catabolic O_2 flux in the NADH-pathway. The H^+_{neg}/P_{\gg} ratio is the inward proton
 434 flux from the inter-membrane space to the negatively (neg) charged matrix space, divided
 435 by the flux of phosphorylation of ADP to ATP. These stoichiometries are not fixed because
 436 of ion leaks and proton slip. Modified from Lemieux *et al.* (2017) and Rich (2013).
 437 (C) OXPHOS coupling: O_2 flux through the catabolic ET-pathway, J_{kO_2} , is coupled
 438 by the H^+ circuit to flux through the phosphorylation-pathway of ADP to ATP, $J_{P_{\gg}}$.
 439 (D) Chemiosmotic phosphorylation-pathway catalyzed by the proton pump F_1F_0 -ATPase
 440 (F-ATPase, ATP synthase), adenine nucleotide translocase (ANT), and inorganic
 441 phosphate carrier (PiC). The H^+_{neg}/P_{\gg} stoichiometry is the sum of the coupling
 442 stoichiometry in the F-ATPase reaction ($-2.7 H^+_{\text{pos}}$ from the positive intermembrane space,
 443 $2.7 H^+_{\text{neg}}$ to the matrix, *i.e.*, the negative compartment) and the proton balance in the
 444 translocation of ADP^{3-} , ATP^{4-} and P_i^{2-} . Modified from Gnaiger (2014).
 445

446 The plasma membrane separates the intracellular compartment including the cytosol, nucleus, and
 447 organelles from the extracellular environment. The plasma membrane consists of a lipid bilayer with
 448 embedded proteins and attached organic molecules that collectively control the selective permeability
 449 of ions, organic molecules, and particles across the cell boundary. The intact plasma membrane prevents
 450 the passage of many water-soluble mitochondrial substrates and inorganic ions—such as succinate,
 451 adenosine diphosphate (ADP) and inorganic phosphate (P_i) that must be precisely controlled at
 452 kinetically-saturating concentrations for the analysis of mitochondrial respiratory capacities.
 453 Respiratory capacities delineate, comparable to channel capacity in information theory (Schneider
 454 2006), the upper boundary of the rate of O_2 consumption measured in defined respiratory states. Despite
 455 the activity of solute carriers, *e.g.*, SLC13A3 and SLC20A2, which transport specific metabolites across
 456 the plasma membrane of various cell types, the intact plasma membrane limits the scope of
 457 investigations into mitochondrial respiratory function in intact cells.

458 **2.1.2. Specification of biochemical dose:** Substrates, uncouplers, inhibitors, and other chemical
 459 reagents are titrated to analyse cellular and mitochondrial function. Nominal concentrations of these
 460 substances are usually reported as initial amount of substance concentration [$\text{mol}\cdot\text{L}^{-1}$] in the incubation
 461 medium. When aiming at the measurement of kinetically saturated processes—such as OXPHOS-
 462 capacities—the concentrations for substrates can be chosen according to the apparent equilibrium
 463 constant, K_m' . In the case of hyperbolic kinetics, only 80% of maximum respiratory capacity is obtained
 464 at a substrate concentration of four times the K_m' , whereas substrate concentrations of 5, 9, 19 and 49
 465 times the K_m' are theoretically required for reaching 83%, 90%, 95% or 98% of the maximal rate
 466 (Gnaiger 2001). Other reagents are chosen to inhibit or alter a particular process. The amount of these
 467 chemicals in an experimental incubation is selected to maximize effect, avoiding unacceptable off-target
 468 consequences that would adversely affect the data being sought. Specifying the amount of substance in
 469 an incubation as nominal concentration in the aqueous incubation medium can be ambiguous (Doskey
 470 *et al.* 2015), particularly for cations (TPP^+ ; fluorescent dyes such as safranin, TMRM; Chowdhury *et al.*
 471 2015) and lipophilic substances (oligomycin, uncouplers, permeabilization agents; Doerrier *et al.* 2018),
 472 which accumulate in the mitochondrial matrix or in biological membranes, respectively. Generally,
 473 dose/exposure can be specified per unit of biological sample, *i.e.*, (nominal moles of
 474 xenobiotic)/(number of cells) [$\text{mol}\cdot\text{cell}^{-1}$] or, as appropriate, per mass of biological sample [$\text{mol}\cdot\text{kg}^{-1}$].
 475 This approach to specification of dose/exposure provides a scalable parameter that can be used to design
 476 experiments, help interpret a wide variety of experimental results, and provide absolute information that
 477 allows researchers worldwide to make the most use of published data (Doskey *et al.* 2015).

478 2.2. Mitochondrial preparations

479

480 Mitochondrial preparations are defined as either isolated mitochondria or tissue and cellular
 481 preparations in which the barrier function of the plasma membrane is disrupted. Since this entails the
 482 loss of cell viability, mitochondrial preparations are not studied *in vivo*. In contrast to isolated
 483 mitochondria and tissue homogenate preparations, mitochondria in permeabilized tissues and cells are
 484 *in situ* relative to the plasma membrane. When studying mitochondrial preparations, substrate-
 485 uncoupler-inhibitor-titration (SUIT) protocols are used to establish respiratory coupling control states
 486 (CCS) and pathway control states (PCS) that provide reference values for various output variables
 487 (**Table 1**). Physiological conditions *in vivo* deviate from these experimentally obtained states; this is
 488 because kinetically-saturating concentrations, *e.g.*, of ADP, oxygen (O₂; dioxygen) or fuel substrates,
 489 may not apply to physiological intracellular conditions. Further information is obtained in studies of
 490 kinetic responses to variations in fuel substrate concentrations, [ADP], or [O₂] in the range between
 491 kinetically-saturating concentrations and anoxia (Gnaiger 2001).

492 The cholesterol content of the plasma membrane is high compared to mitochondrial membranes
 493 (Korn 1969). Therefore, mild detergents—such as digitonin and saponin—can be applied to selectively
 494 permeabilize the plasma membrane via interaction with cholesterol; this allows free exchange of organic
 495 molecules and inorganic ions between the cytosol and the immediate cell environment, while
 496 maintaining the integrity and localization of organelles, cytoskeleton, and the nucleus. Application of
 497 permeabilization agents (mild detergents or toxins) leads to washout of cytosolic marker enzymes—
 498 such as lactate dehydrogenase—and results in the complete loss of cell viability (tested by nuclear
 499 staining using plasma membrane-impermeable dyes), while mitochondrial function remains intact
 500 (tested by cytochrome *c* stimulation of respiration). Digitonin concentrations have to be optimized
 501 according to cell type, particularly since mitochondria from cancer cells contain significantly higher
 502 contents of cholesterol in both membranes (Baggetto and Testa-Perussini, 1990). For example, a dose
 503 of digitonin of 8 fmol·cell⁻¹ (10 pg·cell⁻¹; 10 μg·10⁻⁶ cells) is optimal for permeabilization of endothelial
 504 cells, and the concentration in the incubation medium has to be adjusted according to the cell density
 505 (Doerrier *et al.* 2018). Respiration of isolated mitochondria remains unaltered after the addition of low
 506 concentrations of digitonin or saponin. In addition to mechanical cell disruption during homogenization
 507 of tissue, permeabilization agents may be applied to ensure permeabilization of all cells in tissue
 508 homogenates.

509 Suspensions of cells permeabilized in the respiration chamber and crude tissue homogenates
 510 contain all components of the cell at highly dilute concentrations. All mitochondria are retained in
 511 chemically-permeabilized mitochondrial preparations and crude tissue homogenates. In the preparation
 512 of isolated mitochondria, however, the mitochondria are separated from other cell fractions and purified
 513 by differential centrifugation, entailing the loss of mitochondria at typical recoveries ranging from 30%
 514 to 80% of total mitochondrial content (Lai *et al.* 2018). Using Percoll or sucrose density gradients to
 515 maximize the purity of isolated mitochondria may compromise the mitochondrial yield or structural and
 516 functional integrity. Therefore, mitochondrial isolation protocols need to be optimized according to each
 517 study. The term, *mitochondrial preparation*, neither includes intact cells, nor submitochondrial particles
 518 and further fractionation of mitochondrial components.

519

520 2.3. Electron transfer pathways

521

522 Mitochondrial electron transfer (ET) pathways are fuelled by diffusion and transport of substrates
 523 across the mtOM and mtIM. In addition, the mitochondrial electron transfer system (ETS) consists of
 524 the matrix-ETS and membrane-ETS (**Figure 2B**). Upstream sections of ET-pathways converge at the
 525 NADH-junction (N-junction). NADH is mainly generated in the tricarboxylic acid (TCA) cycle and is
 526 oxidized by Complex I (CI), with further electron entry into the coenzyme Q-junction (Q-junction).
 527 Similarly, succinate is formed in the TCA cycle and oxidized by CII to fumarate. CII is part of both the
 528 TCA cycle and the ETS, and reduces FAD to FADH₂ with further reduction of ubiquinone to ubiquinol
 529 downstream of the TCA cycle in the Q-junction. Thus FADH₂ is not a substrate but is the product of
 530 CII, in contrast to erroneous metabolic maps shown in many publications. β-oxidation of fatty acids
 531 (FA) generates FADH₂ as the substrate of electron transferring flavoprotein complex (ETF).

532 Selected mitochondrial catabolic pathways, *k*, of electron transfer from the oxidation of fuel
 533 substrates to the reduction of O₂ are activated by addition of fuel substrates to the mitochondrial

534 respiration medium after depletion of endogenous substrates (**Figure 2B**). Substrate combinations and
 535 specific inhibitors of ET-pathway enzymes are used to obtain defined pathway control states in
 536 mitochondrial preparations (Gnaiger 2014).

537

538 2.4. Respiratory coupling control

539

540 **2.4.1. Coupling:** In mitochondrial electron transfer, vectorial transmembrane proton flux is
 541 coupled through the redox proton pumps CI, CIII and CIV to the catabolic flux of scalar reactions,
 542 collectively measured as O₂ flux, J_{KO_2} (**Figure 2**). Thus mitochondria are elementary components of
 543 energy transformation. Energy is a conserved quantity and cannot be lost or produced in any internal
 544 process (First Law of Thermodynamics). Open and closed systems can gain or lose energy only by
 545 external fluxes—by exchange with the environment. Therefore, energy can neither be produced by
 546 mitochondria, nor is there any internal process without energy conservation. Exergy or Gibbs energy
 547 ('free energy') is the part of energy that can potentially be transformed into work under conditions of
 548 constant temperature and pressure. *Coupling* is the interaction of an exergonic process (spontaneous,
 549 negative exergy change) with an endergonic process (positive exergy change) in energy transformations
 550 which conserve part of the exergy that would be irreversibly lost or dissipated in an uncoupled process.

551 Pathway control states (PCS) and coupling control states (CCS) are complementary, since
 552 mitochondrial preparations depend on (1) an exogenous supply of pathway-specific fuel substrates and
 553 oxygen, and (2) exogenous control of phosphorylation (**Figure 2**).

554 **2.4.2. Phosphorylation, P», and P»/O₂ ratio:** Phosphorylation in the context of OXPHOS is
 555 defined as phosphorylation of ADP by P_i to form ATP. On the other hand, the term phosphorylation is
 556 used generally in many contexts, *e.g.*, protein phosphorylation. This justifies consideration of a symbol
 557 more discriminating and specific than P as used in the P/O ratio (phosphate to atomic oxygen ratio),
 558 where P indicates phosphorylation of ADP to ATP or GDP to GTP (**Figure 2**). We propose the symbol
 559 P» for the endergonic (uphill) direction of phosphorylation ADP→ATP, and likewise the symbol P« for
 560 the corresponding exergonic (downhill) hydrolysis ATP→ADP. P» refers mainly to electrontransfer
 561 phosphorylation but may also involve substrate-level phosphorylation as part of the TCA cycle
 562 (succinyl-CoA ligase, phosphoglycerate kinase) and phosphorylation of ADP catalyzed by pyruvate
 563 kinase, and of GDP phosphorylated by phosphoenolpyruvate carboxykinase. Transphosphorylation is
 564 performed by adenylate kinase, creatine kinase (mtCK), hexokinase and nucleoside diphosphate kinase.
 565 In isolated mammalian mitochondria, ATP production catalyzed by adenylate kinase (2 ADP ↔ ATP +
 566 AMP) proceeds without fuel substrates in the presence of ADP (Komlódi and Tretter 2017). Kinase
 567 cycles are involved in intracellular energy transfer and signal transduction for regulation of energy flux.

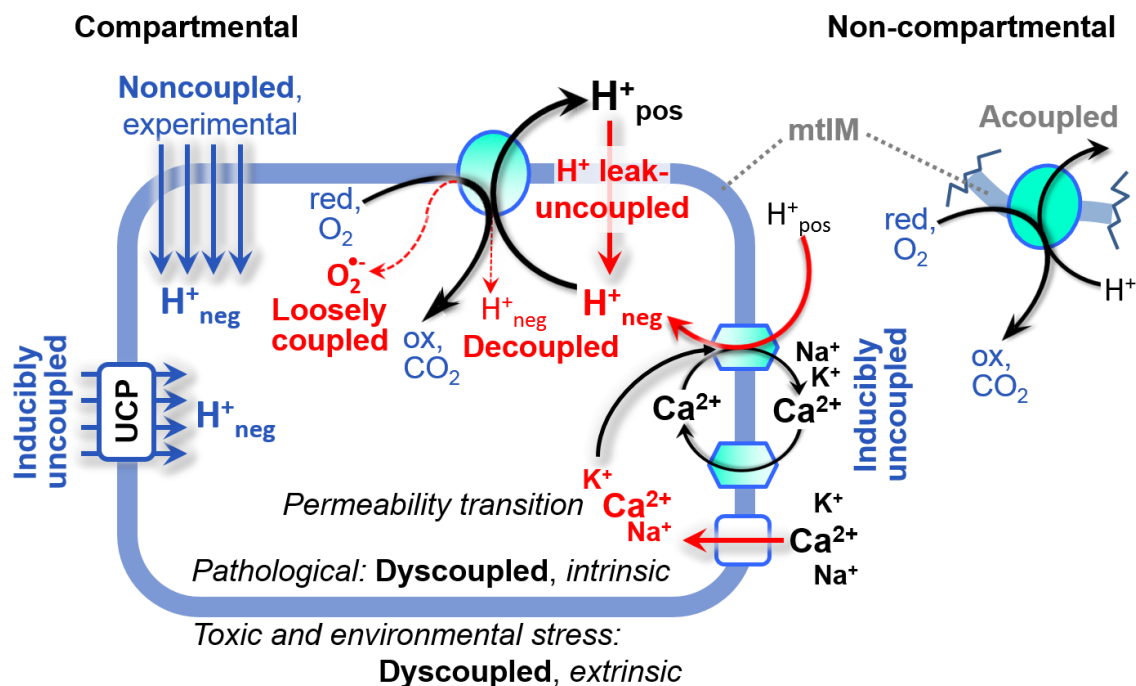
568 The P»/O₂ ratio (P»/4 e⁻) is two times the 'P/O' ratio (P»/2 e⁻). P»/O₂ is a generalized symbol, not
 569 specific for reporting P_i consumption (P_i/O₂ flux ratio), ADP depletion (ADP/O₂ flux ratio), or ATP
 570 production (ATP/O₂ flux ratio). The mechanistic P»/O₂ ratio—or P»/O₂ stoichiometry—is calculated
 571 from the proton-to-O₂ and proton-to-phosphorylation coupling stoichiometries (**Figure 2B**):

$$573 \quad \text{P»/O}_2 = \frac{H_{\text{pos/O}_2}^+}{H_{\text{neg/P»}}^+} \quad (1)$$

574
 575 The H⁺_{pos/O₂} coupling stoichiometry (referring to the full four electron reduction of O₂) depends on the
 576 relative involvement of the three coupling sites (respiratory Complexes CI, CIII and CIV) in the
 577 catabolic ET-pathway from reduced fuel substrates (electron donors) to the reduction of O₂ (electron
 578 acceptor). This varies with: (1) a bypass of CI by single or multiple electron input into the Q-junction;
 579 and (2) a bypass of CIV by involvement of alternative oxidases, AOX. AOX are expressed in all plants,
 580 some fungi, many protists, and several animal phyla, but are not expressed in vertebrate mitochondria
 581 (McDonald *et al.* 2009).

582 The H⁺_{pos/O₂} coupling stoichiometry equals 12 in the ET-pathways involving CIII and CIV as
 583 proton pumps, increasing to 20 for the NADH-pathway through CI (**Figure 2B**), but a general consensus
 584 on H⁺_{pos/O₂} stoichiometries remains to be reached (Hinkle 2005; Wikström and Hummer 2012; Sazanov
 585 2015). The H⁺_{neg/P»} coupling stoichiometry (3.7; **Figure 2B**) is the sum of 2.7 H⁺_{neg} required by the F-
 586 ATPase of vertebrate and most invertebrate species (Watt *et al.* 2010) and the proton balance in the
 587 translocation of ADP, ATP and P_i (**Figure 2C**). Taken together, the mechanistic P»/O₂ ratio is calculated
 588 at 5.4 and 3.3 for NADH- and succinate-linked respiration, respectively (Eq. 1). The corresponding
 589 classical P»/O ratios (referring to the 2 electron reduction of 0.5 O₂) are 2.7 and 1.6 (Watt *et al.* 2010),
 590 in agreement with the measured P»/O ratio for succinate of 1.58 ± 0.02 (Gnaiger *et al.* 2000).

591



592

593

Figure 3. Mechanisms of respiratory uncoupling

594 An intact mitochondrial inner membrane, mtIM, is required for vectorial, compartmental coupling.

595 'Acoupled' respiration is the consequence of structural disruption with catalytic activity of non-

596 compartmental mitochondrial fragments. Inducible uncoupling, *e.g.*, by activation of UCP1, increases

597 LEAK-respiration; experimentally noncoupled respiration provides an estimate of ET-capacity obtained

598 by titration of protonophores stimulating respiration to maximum O_2 flux. H^+ leak-uncoupled,

599 decoupled, and loosely coupled respiration are components of intrinsic uncoupling (Table 2).

600 Pathological dysfunction may affect all types of uncoupling, including permeability transition, causing

601 intrinsically dyscoupled respiration. Similarly, toxicological and environmental stress factors can cause

602 extrinsically dyscoupled respiration. Reduced fuel substrates, red; oxidized products, ox.

603

604 **2.4.3. Uncoupling:** The effective P_{\gg}/O_2 flux ratio ($Y_{P_{\gg}/O_2} = J_{P_{\gg}}/J_{kO_2}$) is diminished relative to the

605 mechanistic P_{\gg}/O_2 ratio by intrinsic and extrinsic uncoupling or dyscoupling (Figure 3). Such

606 generalized uncoupling is different from switching to mitochondrial pathways that involve fewer than

607 three proton pumps ('coupling sites': Complexes CI, CIII and CIV), bypassing CI through multiple

608 electron entries into the Q-junction, or CIII and CIV through AOX (Figure 2B). Reprogramming of

609 mitochondrial pathways leading to different types of substrates being oxidized may be considered as a

610 switch of gears (changing the stoichiometry by altering the substrate that is oxidized) rather than

611 uncoupling (loosening the tightness of coupling relative to a fixed stoichiometry). In addition, Y_{P_{\gg}/O_2}

612 depends on several experimental conditions of flux control, increasing as a hyperbolic function of [ADP]

613 to a maximum value (Gnaiger 2001).

614 Uncoupling of mitochondrial respiration is a general term comprising diverse mechanisms:

615 1. Proton leak across the mtIM from the positive to the negative compartment (H^+ leak-uncoupled;

616 **Figure 3).**

617 2. Cycling of other cations, strongly stimulated by permeability transition; comparable to the use of

618 protonophores, cation cycling is experimentally induced by valinomycin in the presence of K^+ ;

619 3. Decoupling by proton slip in the redox proton pumps when protons are effectively not pumped

620 (CI, CIII and CIV) or are not driving phosphorylation (F-ATPase);

621 4. Loss of vesicular (compartmental) integrity when electron transfer is acoupled;

622 5. Electron leak in the loosely coupled univalent reduction of O_2 to superoxide ($O_2^{\cdot-}$; superoxide

623 anion radical).

624 Differences of terms—uncoupled *vs.* noncoupled—are easily overlooked, although they relate to

625 different meanings of uncoupling (Figure 3 and Table 2).

626

627 2.5. Coupling states and respiratory rates

628

629

630

631

632

633

634

635

636

637

638

639

640

To extend the classical nomenclature on mitochondrial coupling states (Section 2.6) by a concept-driven terminology that explicitly incorporates information on the meaning of respiratory states, the terminology must be general and not restricted to any particular experimental protocol or mitochondrial preparation (Gnaiger 2009). Concept-driven nomenclature aims at mapping the meaning and concept behind the words and acronyms onto the forms of words and acronyms (Miller 1991). The focus of concept-driven nomenclature is primarily the conceptual *why*, along with clarification of the experimental *how*.

Table 1. Coupling states and residual oxygen consumption in mitochondrial preparations in relation to respiration- and phosphorylation-flux, J_{KO_2} and J_{P} , and protonmotive force, pmf. Coupling states are established at kinetically-saturating concentrations of fuel substrates and O_2 .

State	J_{KO_2}	J_{P}	pmf	Inducing factors	Limiting factors
LEAK	L ; low, cation leak-dependent respiration	0	max.	back-flux of cations including proton leak, proton slip	$J_{\text{P}} = 0$: (1) without ADP, L_{N} ; (2) max. ATP/ADP ratio, L_{T} ; or (3) inhibition of the phosphorylation-pathway, L_{omy}
OXPHOS	P ; high, ADP-stimulated respiration, OXPHOS-capacity	max.	high	kinetically-saturating [ADP] and $[\text{P}_i]$	J_{P} by phosphorylation-pathway capacity; or J_{KO_2} by ET-capacity
ET	E ; max., noncoupled respiration, ET-capacity	0	low	optimal external uncoupler concentration for max. $J_{\text{O}_2, \text{E}}$	J_{KO_2} by ET-capacity
ROX	R_{ox} ; min., residual O_2 consumption	0	0	$J_{\text{O}_2, \text{Rox}}$ in non-ET-pathway oxidation reactions	inhibition of all ET-pathways; or absence of fuel substrates

641

642

643

644

645

646

647

648

649

650

651

652

653

654

655

656

657

658

659

660

661

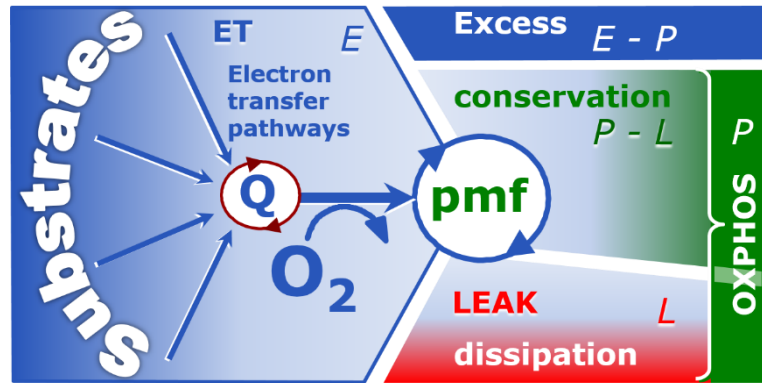
662

To provide a diagnostic reference for respiratory capacities of core energy metabolism, the capacity of oxidative phosphorylation, OXPHOS, is measured at kinetically-saturating concentrations of ADP and P_i . The oxidative ET-capacity reveals the limitation of OXPHOS-capacity mediated by the phosphorylation-pathway. The ET- and phosphorylation-pathways comprise coupled segments of the OXPHOS-system. By application of external uncouplers, ET-capacity is measured as noncoupled respiration. The contribution of intrinsically uncoupled O_2 consumption is studied by preventing the stimulation of phosphorylation either in the absence of ADP or by inhibition of the phosphorylation-pathway. The corresponding states are collectively classified as LEAK-states when O_2 consumption compensates mainly for ion leaks, including the proton leak. Defined coupling states are induced by: (1) adding cation chelators such as EGTA, binding free Ca^{2+} and thus limiting cation cycling; (2) adding ADP and P_i ; (3) inhibiting the phosphorylation-pathway; and (4) uncoupler titrations, while maintaining a defined ET-pathway state with constant fuel substrates and inhibitors of specific branches of the ET-pathway.

The three coupling states, ET, LEAK and OXPHOS, are shown schematically with the corresponding respiratory rates, abbreviated as E , L and P , respectively (**Figure 4**). We distinguish metabolic *pathways* from metabolic *states* and the corresponding metabolic *rates*; for example: ET-pathways, ET-states, and ET-capacities, E , respectively (**Table 1**). The protonmotive force is *high* in the OXPHOS-state when it drives phosphorylation, *maximum* in the LEAK-state of coupled mitochondria, driven by LEAK-respiration at a minimum back-flux of cations to the matrix side, and *very low* in the ET-state when uncouplers short-circuit the proton cycle (**Table 1**).

663 **Figure 4. Four-compartment**
 664 **model of oxidative**
 665 **phosphorylation**

666 Respiratory states (ET, OXPHOS,
 667 LEAK; Table 1) and corresponding
 668 rates (E , P , L) are connected by the
 669 protonmotive force, pmf. (1) ET-
 670 capacity, E , is partitioned into (2)
 671 dissipative LEAK-respiration, L ,
 672 when the Gibbs energy change of
 673 catabolic O_2 flux is irreversibly lost,
 674 (3) net OXPHOS-capacity, $P-L$, with
 675 partial conservation of the capacity to perform work, and (4) the excess capacity, $E-P$. Modified from
 676 Gnaiger (2014).

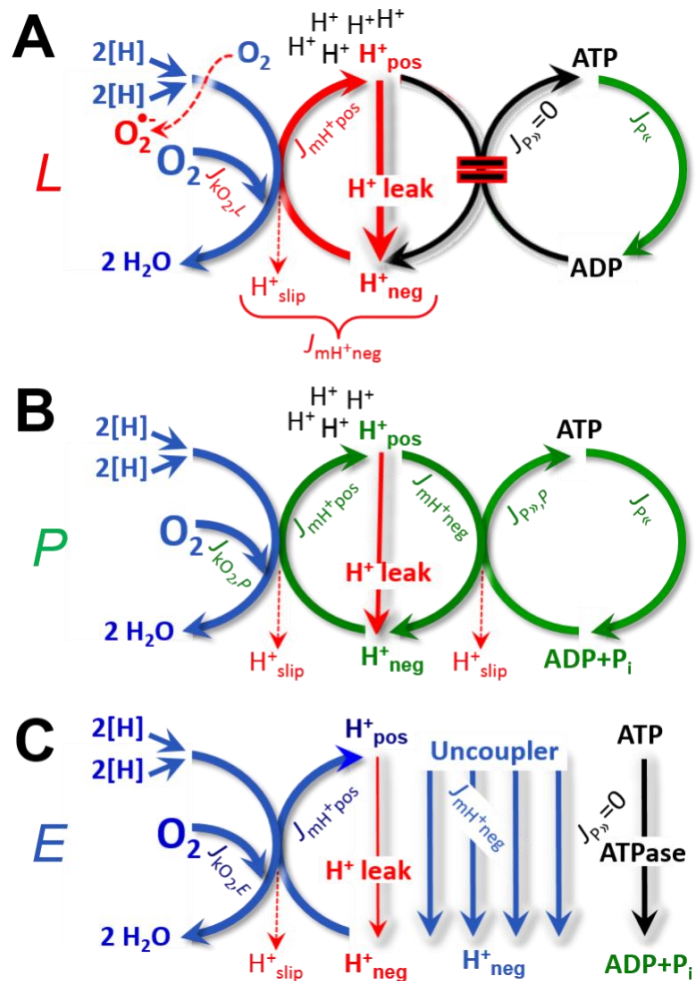


677 **Figure 5. Respiratory coupling**
 678 **states**

679 (A) **LEAK-state and rate, L** :
 680 Oxidation only, since phosphorylation
 681 is arrested, $J_{P\gg} = 0$, and catabolic O_2
 682 flux, $J_{kO_2,L}$, is controlled mainly by the
 683 proton leak and slip, J_{mH^+neg} , at
 684 maximum protonmotive force (Figure
 685 4). Extramitochondrial ATP may be
 686 hydrolyzed by extramitochondrial
 ATPases, $J_{P\ll}$; then phosphorylation
 must be blocked.

(B) **OXPHOS-state and rate, P** :
 Oxidation coupled to
 phosphorylation, $J_{P\gg}$, which is
 stimulated by kinetically-saturating
 [ADP] and $[P_i]$, supported by a high
 protonmotive force. O_2 flux, $J_{kO_2,P}$, is
 well-coupled at a $P\gg/O_2$ ratio of
 $J_{P\gg,P}/J_{O_2,P}$. Extramitochondrial
 ATPases may recycle ATP, $J_{P\ll}$.

(C) **ET-state and rate, E** : Oxidation
 only, since phosphorylation is zero,
 $J_{P\gg} = 0$, at optimum exogenous
 uncoupler concentration when
 noncoupled respiration, $J_{kO_2,E}$, is
 maximum. The F-ATPase may
 hydrolyze extramitochondrial ATP.



677

678 **2.5.1. LEAK-state (Figure 5A):** The LEAK-state is defined as a state of mitochondrial
 679 respiration when O_2 flux mainly compensates for ion leaks in the absence of ATP synthesis, at
 680 kinetically-saturating concentrations of O_2 , respiratory fuel substrates and P_i . LEAK-respiration is
 681 measured to obtain an estimate of intrinsic uncoupling without addition of an experimental uncoupler:
 682 (1) in the absence of adenylates, *i.e.*, AMP, ADP and ATP; (2) after depletion of ADP at a maximum
 683 ATP/ADP ratio; or (3) after inhibition of the phosphorylation-pathway by inhibitors of F-ATPase—such
 684 as oligomycin, or of adenine nucleotide translocase—such as carboxyatractylsido. Adjustment of the
 685 nominal concentration of these inhibitors to the density of biological sample applied can minimize or
 686 avoid inhibitory side-effects exerted on ET-capacity or even some dyscoupling.

687

Table 2. Terms on respiratory coupling and uncoupling.

Term	J_{kO_2}	$P \gg O_2$	Notes	
acoupled		0	electron transfer in mitochondrial fragments without vectorial proton translocation (Figure 3)	
intrinsic, no protonophore added	uncoupled	L	0	non-phosphorylating LEAK-respiration (Figure 5A)
	proton leak-uncoupled		0	component of L , H^+ diffusion across the mtIM (Figure 3)
	decoupled		0	component of L , proton slip (Figure 3)
	loosely coupled		0	component of L , lower coupling due to superoxide formation and bypass of proton pumps by electron leak (Figure 3)
	dyscoupled		0	pathologically, toxicologically, environmentally increased uncoupling, mitochondrial dysfunction
	inducibly uncoupled		0	by UCP1 or cation (<i>e.g.</i> , Ca^{2+}) cycling (Figure 3)
noncoupled	E	0	ET-capacity, non-phosphorylating respiration stimulated to maximum flux at optimum exogenous protonophore concentration (Figure 5C)	
well-coupled	P	high	OXPHOS-capacity , phosphorylating respiration with an intrinsic LEAK component (Figure 5B)	
fully coupled	$P - L$	max.	OXPHOS-capacity corrected for LEAK-respiration (Figure 4)	

688

689

690

691

692

693

694

695

696

697

698

699

700

701

702

703

704

705

706

707

708

709

710

711

712

713

714

715

- **Proton leak and uncoupled respiration:** The intrinsic proton leak is the *uncoupled* leak current of protons in which protons diffuse across the mtIM in the dissipative direction of the downhill protonmotive force without coupling to phosphorylation (**Figure 5A**). The proton leak flux depends non-linearly on the protonmotive force (Garlid *et al.* 1989; Divakaruni and Brand 2011), which is a temperature-dependent property of the mtIM and may be enhanced due to possible contamination by free fatty acids. Inducible uncoupling mediated by uncoupling protein 1 (UCP1) is physiologically controlled, *e.g.*, in brown adipose tissue. UCP1 is a member of the mitochondrial carrier family that is involved in the translocation of protons across the mtIM (Klingenberg 2017). Consequently, this short-circuit lowers the protonmotive force and stimulates electron transfer, respiration, and heat dissipation in the absence of phosphorylation of ADP.
- **Cation cycling:** There can be other cation contributors to leak current including calcium and probably magnesium. Calcium influx is balanced by mitochondrial Na^+/Ca^{2+} or H^+/Ca^{2+} exchange, which is balanced by Na^+/H^+ or K^+/H^+ exchanges. This is another effective uncoupling mechanism different from proton leak (**Table 2**).
- **Proton slip and decoupled respiration:** Proton slip is the *decoupled* process in which protons are only partially translocated by a redox proton pump of the ET-pathways and slip back to the original vesicular compartment. The proton leak is the dominant contributor to the overall leak current in mammalian mitochondria incubated under physiological conditions at 37 °C, whereas proton slip increases at lower experimental temperature (Canton *et al.* 1995). Proton slip can also happen in association with the F-ATPase, in which the proton slips downhill across the pump to the matrix without contributing to ATP synthesis. In each case, proton slip is a property of the proton pump and increases with the pump turnover rate.
- **Electron leak and loosely coupled respiration:** Superoxide production by the ETS leads to a bypass of redox proton pumps and correspondingly lower $P \gg O_2$ ratio. This depends on the actual site of electron leak and the scavenging of hydrogen peroxide by cytochrome *c*, whereby electrons may re-enter the ETS with proton translocation by CIV.

- **Loss of compartmental integrity and acoupled respiration:** Electron transfer and catabolic O₂ flux proceed without compartmental proton translocation in disrupted mitochondrial fragments. Such fragments are an artefact of mitochondrial isolation, and may not fully fuse to re-establish structurally intact mitochondria. Loss of mtIM integrity, therefore, is the cause of acoupled respiration, which is a nonvectorial dissipative process without control by the protonmotive force.
- **Dyscoupled respiration:** Mitochondrial injuries may lead to *dyscoupling* as a pathological or toxicological cause of *uncoupled* respiration. Dyscoupling may involve any type of uncoupling mechanism, *e.g.*, opening the permeability transition pore. Dyscoupled respiration is distinguished from the experimentally induced *noncoupled* respiration in the ET-state (**Table 2**).

2.5.2. OXPHOS-state (Figure 5B): The OXPHOS-state is defined as the respiratory state with kinetically-saturating concentrations of O₂, respiratory and phosphorylation substrates, and absence of exogenous uncoupler, which provides an estimate of the maximal respiratory capacity in the OXPHOS-state for any given ET-pathway state. Respiratory capacities at kinetically-saturating substrate concentrations provide reference values or upper limits of performance, aiming at the generation of data sets for comparative purposes. Physiological activities and effects of substrate kinetics can be evaluated relative to the OXPHOS-capacity.

As discussed previously, 0.2 mM ADP does not fully saturate flux in isolated mitochondria (Gnaiger 2001; Puchowicz *et al.* 2004); greater [ADP] is required, particularly in permeabilized muscle fibres and cardiomyocytes, to overcome limitations by intracellular diffusion and by the reduced conductance of the mtOM (Jepihhina *et al.* 2011; Illaste *et al.* 2012; Simson *et al.* 2016), either through interaction with tubulin (Rostovtseva *et al.* 2008) or other intracellular structures (Birkedal *et al.* 2014). In addition, saturating ADP concentrations need to be evaluated under different experimental conditions such as temperature (Lemieux *et al.* 2017) and with different animal models (Blier and Guderley, 1993). In permeabilized muscle fibre bundles of high respiratory capacity, the apparent K_m for ADP increases up to 0.5 mM (Saks *et al.* 1998), consistent with experimental evidence that >90% saturation is reached only at >5 mM ADP (Pesta and Gnaiger 2012). Similar ADP concentrations are also required for accurate determination of OXPHOS-capacity in human clinical cancer samples and permeabilized cells (Klepinin *et al.* 2016; Koit *et al.* 2017). 2.5 to 5 mM ADP is sufficient to obtain the actual OXPHOS-capacity in many types of permeabilized tissue and cell preparations, but experimental validation is required in each specific case.

2.5.3. Electron transfer-state (Figure 5C): O₂ flux determined in the ET-state yields an estimate of ET-capacity. The ET-state is defined as the *noncoupled* state with kinetically-saturating concentrations of O₂, respiratory substrate and optimum exogenous uncoupler concentration for maximum O₂ flux. Uncouplers are weak lipid-soluble acids which function as protonophores. These disrupt the barrier function of the mtIM and thus short circuit the protonmotive system, functioning like a clutch in a mechanical system. As a consequence of the nearly collapsed protonmotive force, the driving force is insufficient for phosphorylation, and $J_{P_s} = 0$. The most frequently used uncouplers are carbonyl cyanide *m*-chloro phenyl hydrazone (CCCP), carbonyl cyanide *p*-trifluoromethoxyphenylhydrazone (FCCP), or dinitrophenol (DNP). Stepwise titration of uncouplers stimulates respiration up to or above the level of O₂ consumption rates in the OXPHOS-state; respiration is inhibited, however, above optimum uncoupler concentrations (Mitchell 2011). Data obtained with a single dose of uncoupler must be evaluated with caution, particularly when a fixed uncoupler concentration is used in studies exploring a treatment or disease that may alter the mitochondrial content or mitochondrial sensitivity to inhibition by uncouplers. The effect on ET-capacity of the reversed function of F-ATPase (J_{P_r} ; **Figure 5C**) can be evaluated in the presence and absence of extramitochondrial ATP.

2.5.4. ROX state and Rox: Besides the three fundamental coupling states of mitochondrial preparations, the state of residual O₂ consumption, ROX, which although not a coupling state, is relevant to assess respiratory function (**Figure 1**). The rate of residual oxygen consumption, *Rox*, is defined as O₂ consumption due to oxidative reactions measured after inhibition of ET with rotenone, malonic acid and antimycin A. Cyanide and azide inhibit not only CIV but catalase and several peroxidases involved in *Rox*. High concentrations of antimycin A, but not rotenone or cyanide, inhibit peroxisomal acyl-CoA oxidase and D-amino acid oxidase (Vamecq *et al.* 1987). *Rox* represents a baseline used to correct respiration measured in defined coupling control states. *Rox*-corrected *L*, *P* and *E* not only lower the values of total fluxes, but also change the flux control ratios *L/P* and *L/E*. *Rox* is not necessarily

772 equivalent to non-mitochondrial reduction of O₂, considering O₂-consuming reactions in mitochondria
 773 that are not related to ET—such as O₂ consumption in reactions catalyzed by monoamine oxidases (type
 774 A and B), monooxygenases (cytochrome P450 monooxygenases), dioxygenase (sulfur dioxygenase and
 775 trimethyllysine dioxygenase), and several hydroxylases. Even isolated mitochondrial fractions,
 776 especially those obtained from liver, may be contaminated by peroxisomes, as shown by transmission
 777 electron microscopy. This fact makes the exact determination of mitochondrial O₂ consumption and
 778 mitochondria-associated generation of reactive oxygen species complicated (Schönfeld *et al.* 2009;
 779 Speijer 2016; **Figure 2**). The dependence of ROX-linked O₂ consumption needs to be studied in detail
 780 together with non-ET enzyme activities, availability of specific substrates, O₂ concentration, and
 781 electron leakage leading to the formation of reactive oxygen species.

782 **2.5.5. Quantitative relations:** E may exceed or be equal to P . $E > P$ is observed in many types
 783 of mitochondria, varying between species, tissues and cell types (Gnaiger 2009). $E - P$ is the excess ET-
 784 capacity pushing the phosphorylation-flux (**Figure 2C**) to the limit of its capacity for utilizing the
 785 protonmotive force. In addition, the magnitude of $E - P$ depends on the tightness of respiratory coupling
 786 or degree of uncoupling, since an increase of L causes P to increase towards the limit of E . The *excess*
 787 $E - P$ capacity, $E - P$, therefore, provides a sensitive diagnostic indicator of specific injuries of the
 788 phosphorylation-pathway, under conditions when E remains constant but P declines relative to controls
 789 (**Figure 4**). Substrate cocktails supporting simultaneous convergent electron transfer to the Q-junction
 790 for reconstitution of TCA cycle function establish pathway control states with high ET-capacity, and
 791 consequently increase the sensitivity of the $E - P$ assay.

792 E cannot theoretically be lower than P . $E < P$ must be discounted as an artefact, which may be
 793 caused experimentally by: (1) loss of oxidative capacity during the time course of the respirometric
 794 assay, since E is measured subsequently to P ; (2) using insufficient uncoupler concentrations; (3) using
 795 high uncoupler concentrations which inhibit ET (Gnaiger 2008); (4) high oligomycin concentrations
 796 applied for measurement of L before titrations of uncoupler, when oligomycin exerts an inhibitory effect
 797 on E . On the other hand, the excess ET-capacity is overestimated if non-saturating [ADP] or [P_i] are
 798 used. See State 3 in the next section.

799 The net OXPHOS-capacity is calculated by subtracting L from P (**Figure 4**). The net P»/O₂ equals
 800 P»/($P - L$), wherein the dissipative LEAK component in the OXPHOS-state may be overestimated. This
 801 can be avoided by measuring LEAK-respiration in a state when the protonmotive force is adjusted to its
 802 slightly lower value in the OXPHOS-state by titration of an ET inhibitor (Divakaruni and Brand 2011).
 803 Any turnover-dependent components of proton leak and slip, however, are underestimated under these
 804 conditions (Garlid *et al.* 1993). In general, it is inappropriate to use the term *ATP production* or *ATP*
 805 *turnover* for the difference of O₂ flux measured in the OXPHOS and LEAK states. $P - L$ is the upper limit
 806 of OXPHOS-capacity that is freely available for ATP production (corrected for LEAK-respiration) and
 807 is fully coupled to phosphorylation with a maximum mechanistic stoichiometry (**Figure 4**).

808 LEAK-respiration and OXPHOS-capacity depend on (1) the tightness of coupling under the
 809 influence of the respiratory uncoupling mechanisms (**Figure 3**), and (2) the coupling stoichiometry,
 810 which varies as a function of the substrate type undergoing oxidation in ET-pathways with either two
 811 or three coupling sites (**Figure 2B**). When cocktails with NADH-linked substrates and succinate are
 812 used, the relative contribution of ET-pathways with three or two coupling sites cannot be controlled
 813 experimentally, is difficult to determine, and may shift in transitions between LEAK-, OXPHOS- and
 814 ET-states (Gnaiger 2014). Under these experimental conditions, we cannot separate the tightness of
 815 coupling *versus* coupling stoichiometry as the mechanisms of respiratory control in the shift of L/P
 816 ratios. The tightness of coupling and fully coupled O₂ flux, $P - L$ (**Table 2**), therefore, are obtained from
 817 measurements of coupling control of LEAK-respiration, OXPHOS- and ET-capacities in well-defined
 818 pathway states, using either pyruvate and malate as substrates or the classical succinate and rotenone
 819 substrate-inhibitor combination (**Figure 2B**).

820 **2.5.6. The steady-state:** Mitochondria represent a thermodynamically open system in non-
 821 equilibrium states of biochemical energy transformation. State variables (protonmotive force; redox
 822 states) and metabolic *rates* (fluxes) are measured in defined mitochondrial respiratory *states*. Steady-
 823 states can be obtained only in open systems, in which changes by internal transformations, *e.g.*, O₂
 824 consumption, are instantaneously compensated for by external fluxes, *e.g.*, O₂ supply, preventing a
 825 change of O₂ concentration in the system (Gnaiger 1993b). Mitochondrial respiratory states monitored
 826 in closed systems satisfy the criteria of pseudo-steady states for limited periods of time, when changes
 827 in the system (concentrations of O₂, fuel substrates, ADP, P_i, H⁺) do not exert significant effects on

828 metabolic fluxes (respiration, phosphorylation). Such pseudo-steady states require respiratory media
 829 with sufficient buffering capacity and substrates maintained at kinetically-saturating concentrations, and
 830 thus depend on the kinetics of the processes under investigation.

831

832 2.6. Classical terminology for isolated mitochondria

833 'When a code is familiar enough, it ceases appearing like a code; one forgets that there is a
 834 decoding mechanism. The message is identical with its meaning' (Hofstadter 1979).

835

836 Chance and Williams (1955; 1956) introduced five classical states of mitochondrial respiration
 837 and cytochrome redox states. **Table 3** shows a protocol with isolated mitochondria in a closed
 838 respirometric chamber, defining a sequence of respiratory states. States and rates are not specifically
 839 distinguished in this nomenclature.

840

841

Table 3. Metabolic states of mitochondria (Chance and Williams, 1956; Table V).

842

843

State	[O ₂]	ADP level	Substrate level	Respiration rate	Rate-limiting substance
1	>0	low	low	slow	ADP
2	>0	high	~0	slow	substrate
3	>0	high	high	fast	respiratory chain
4	>0	low	high	slow	ADP
5	0	high	high	0	oxygen

844

845

846 **2.6.1. State 1** is obtained after addition of isolated mitochondria to air-saturated
 847 isoosmotic/isotonic respiration medium containing P_i, but no fuel substrates and no adenylates.

848 **2.6.2. State 2** is induced by addition of a 'high' concentration of ADP (typically 100 to 300 μM),
 849 which stimulates respiration transiently on the basis of endogenous fuel substrates and phosphorylates
 850 only a small portion of the added ADP. State 2 is then obtained at a low respiratory activity limited by
 851 exhausted endogenous fuel substrate availability (**Table 3**). If addition of specific inhibitors of
 852 respiratory complexes such as rotenone does not cause a further decline of O₂ flux, State 2 is equivalent
 853 to the ROX state (See below.). If inhibition is observed, undefined endogenous fuel substrates are a
 854 confounding factor of pathway control, contributing to the effect of subsequently externally added
 855 substrates and inhibitors. In contrast to the original protocol, an alternative sequence of titration steps is
 856 frequently applied, in which the alternative 'State 2' has an entirely different meaning when this second
 857 state is induced by addition of fuel substrate without ADP or ATP (LEAK-state; in contrast to State 2
 858 defined in **Table 1** as a ROX state). Some researchers have called this condition as 'pseudostate 4'
 859 because it has no significant concentrations of adenine nucleotides and hence it is not a near-
 860 physiological condition, although it should be used for calculating the net OXPHOS-capacity, *P-L*.

861 **2.6.3. State 3** is the state stimulated by addition of fuel substrates while the ADP concentration
 862 is still high (**Table 3**) and supports coupled energy transformation through oxidative phosphorylation.
 863 'High ADP' is a concentration of ADP specifically selected to allow the measurement of State 3 to State
 864 4 transitions of isolated mitochondria in a closed respirometric chamber. Repeated ADP titration re-
 865 establishes State 3 at 'high ADP'. Starting at O₂ concentrations near air-saturation (193 or 238 μM O₂
 866 at 37 °C or 25 °C and sea level at 1 atm or 101.32 kPa, and an oxygen solubility of respiration medium
 867 at 0.92 times that of pure water; Forstner and Gnaiger 1983), the total ADP concentration added must
 868 be low enough (typically 100 to 300 μM) to allow phosphorylation to ATP at a coupled O₂ flux that
 869 does not lead to O₂ depletion during the transition to State 4. In contrast, kinetically-saturating ADP
 870 concentrations usually are 10-fold higher than 'high ADP', e.g., 2.5 mM in isolated mitochondria. The
 871 abbreviation State 3u is occasionally used in bioenergetics, to indicate the state of respiration after
 872 titration of an uncoupler, without sufficient emphasis on the fundamental difference between OXPHOS-
 873 capacity (*well-coupled* with an endogenous uncoupled component) and ET-capacity (*noncoupled*).

874 **2.6.4. State 4** is a LEAK-state that is obtained only if the mitochondrial preparation is intact and
 875 well-coupled. Depletion of ADP by phosphorylation to ATP causes a decline of O₂ flux in the transition
 876 from State 3 to State 4. Under the conditions of State 4, a maximum protonmotive force and high
 877 ATP/ADP ratio are maintained. The gradual decline of $Y_{P\gg/O_2}$ towards diminishing [ADP] at State 4 must
 878 be taken into account for calculation of $P\gg/O_2$ ratios (Gnaiger 2001). State 4 respiration, L_T (**Table 1**),
 879 reflects intrinsic proton leak and ATP hydrolysis activity. O₂ flux in State 4 is an overestimation of
 880 LEAK-respiration if the contaminating ATP hydrolysis activity recycles some ATP to ADP, $J_{P\ll}$, which
 881 stimulates respiration coupled to phosphorylation, $J_{P\gg} > 0$. Some degree of mechanical disruption and
 882 loss of mitochondrial integrity allows the exposed mitochondrial F-ATPases to hydrolyze the ATP
 883 synthesized by the fraction of coupled mitochondria. This can be tested by inhibition of the
 884 phosphorylation-pathway using oligomycin, ensuring that $J_{P\gg} = 0$ (State 4o). On the other hand, the State
 885 4 respiration reached after exhaustion of added ADP is a more physiological condition, *i.e.*, presence of
 886 ATP, ADP and even AMP. Sequential ADP titrations re-establish State 3, followed by State 3 to State
 887 4 transitions while sufficient O₂ is available. Anoxia may be reached, however, before exhaustion of
 888 ADP (State 5).

889 **2.6.5. State 5** ‘*may be obtained by antimycin A treatment or by anaerobiosis*’ (Chance and
 890 Williams, 1955) ‘. These definitions give State 5 two different meanings of ROX or anoxia, respectively.
 891 Anoxia is obtained after exhaustion of O₂ in a closed respirometric chamber. Diffusion of O₂ from the
 892 surroundings into the aqueous solution may be a confounding factor preventing complete anoxia
 893 (Gnaiger 2001).

894 In **Table 3**, only States 3 and 4 are coupling control states, with the restriction that rates in State
 895 3 may be limited kinetically by non-saturating ADP concentrations.

896

897 2.7. Control and regulation

898

899 The terms metabolic *control* and *regulation* are frequently used synonymously, but are
 900 distinguished in metabolic control analysis: “We could understand the regulation as the mechanism that
 901 occurs when a system maintains some variable constant over time, in spite of fluctuations in external
 902 conditions (homeostasis of the internal state). On the other hand, metabolic control is the power to
 903 change the state of the metabolism in response to an external signal” (Fell 1997). Respiratory control
 904 may be induced by experimental control signals that exert an influence on: (1) ATP demand and ADP
 905 phosphorylation-rate; (2) fuel substrate composition, pathway competition; (3) available amounts of
 906 substrates and O₂, *e.g.*, starvation and hypoxia; (4) the protonmotive force, redox states, flux–force
 907 relationships, coupling and efficiency; (5) Ca²⁺ and other ions including H⁺; (6) inhibitors, *e.g.*, nitric
 908 oxide or intermediary metabolites such as oxaloacetate; (7) signalling pathways and regulatory proteins,
 909 *e.g.*, insulin resistance, transcription factor hypoxia inducible factor 1.

910 Mechanisms of respiratory control and regulation include adjustments of: (1) enzyme activities
 911 by allosteric mechanisms and phosphorylation; (2) enzyme content, concentrations of cofactors and
 912 conserved moieties such as adenylates, nicotinamide adenine dinucleotide [NAD⁺/NADH], coenzyme
 913 Q, cytochrome *c*; (3) metabolic channeling by supercomplexes; and (4) mitochondrial density (enzyme
 914 concentrations and membrane area) and morphology (cristae folding, fission and fusion). Mitochondria
 915 are targeted directly by hormones, *e.g.*, progesterone and glucacorticoids, which affect their energy
 916 metabolism (Lee *et al.* 2013; Gerö and Szabo 2016; Price and Dai 2016; Moreno *et al.* 2017).
 917 Evolutionary or acquired differences in the genetic and epigenetic basis of mitochondrial function (or
 918 dysfunction) between individuals; age; biological sex, and hormone concentrations; life style including
 919 exercise and nutrition; and environmental issues including thermal, atmospheric, toxic and
 920 pharmacological factors, exert an influence on all control mechanisms listed above. For reviews, see
 921 Brown 1992; Gnaiger 1993a, 2009; 2014; Paradies *et al.* 2014; Morrow *et al.* 2017.

922 Lack of control by a metabolic pathway, *e.g.*, phosphorylation-pathway, means that there will
 923 be no response to a variable activating it, *e.g.*, [ADP]. The reverse, however, is not true as the absence
 924 of a response to [ADP] does not exclude the phosphorylation-pathway from having some degree of
 925 control. The degree of control of a component of the OXPHOS-pathway on an output variable, such as
 926 O₂ flux, will in general be different from the degree of control on other outputs, such as phosphorylation-
 927 flux or proton leak flux. Therefore, it is necessary to be specific as to which input and output are under
 928 consideration (Fell 1997).

929 Respiratory control refers to the ability of mitochondria to adjust O₂ flux in response to external
 930 control signals by engaging various mechanisms of control and regulation. Respiratory control is
 931 monitored in a mitochondrial preparation under conditions defined as respiratory states, preferentially
 932 under near-physiological conditions of temperature, pH, and medium ionic composition, to generate
 933 data of higher biological relevance. When phosphorylation of ADP to ATP is stimulated or depressed,
 934 an increase or decrease is observed in electron transfer measured as O₂ flux in respiratory coupling states
 935 of intact mitochondria ('controlled states' in the classical terminology of bioenergetics). Alternatively,
 936 coupling of electron transfer with phosphorylation is diminished by uncouplers. The corresponding
 937 coupling control state is characterized by a high respiratory rate without control by P» (noncoupled or
 938 'uncontrolled state').

939
 940

941 3. What is a rate?

942

943 The term *rate* is not adequately defined to be useful for reporting data. Normalization of 'rates'
 944 leads to a diversity of formats. Application of common and defined units is required for direct transfer
 945 of reported results into a database. The second [s] is the SI unit for the base quantity *time*. It is also the
 946 standard time-unit used in solution chemical kinetics.

947 The inconsistency of the meanings of rate becomes apparent when considering Galileo Galilei's
 948 famous principle, that 'bodies of different weight all fall at the same rate (have a constant acceleration)'
 949 (Coopersmith 2010). A rate may be an extensive quantity, which is a *flow*, *I*, when expressed per object
 950 (per number of cells or organisms) or per chamber (per system). 'System' is defined as the open or
 951 closed chamber of the measuring device. A rate is a *flux*, *J*, when expressed as a size-specific quantity
 952 (Figure 6A; Box 2).

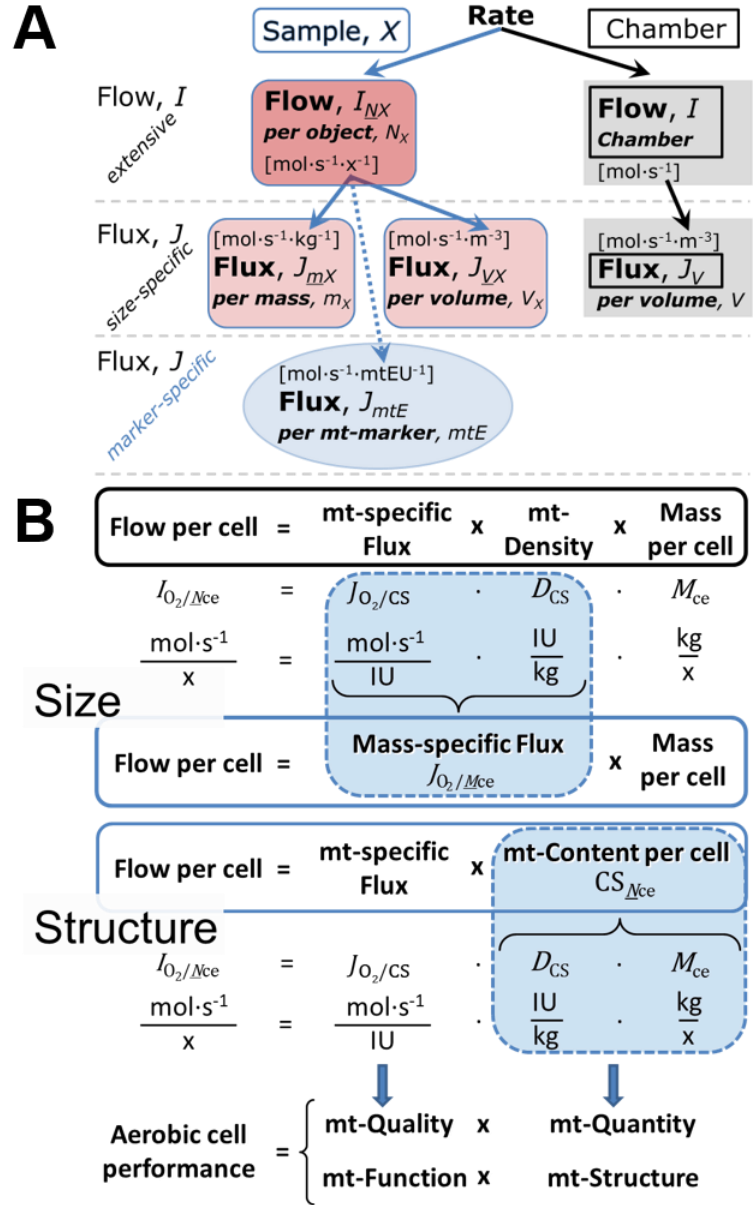
- 953 • **Extensive quantities:** An extensive quantity increases proportionally with system size. For
 954 example, mass and volume are extensive quantities. Flow is an extensive quantity. The
 955 magnitude of an extensive quantity is completely additive for non-interacting subsystems.
 956 The magnitude of these quantities depends on the extent or size of the system (Cohen *et al.*
 957 2008).
- 958 • **Size-specific quantities:** 'The adjective *specific* before the name of an extensive quantity is
 959 often used to mean *divided by mass*' (Cohen *et al.* 2008). In this system-paradigm, mass-
 960 specific flux is flow divided by mass of the system (the total mass of everything within the
 961 measuring chamber or reactor). Rates are frequently expressed as volume-specific flux. A
 962 mass-specific or volume-specific quantity is independent of the extent of non-interacting
 963 homogenous subsystems. Tissue-specific quantities (related to the *sample* in contrast to the
 964 *system*) are of fundamental interest in the field of comparative mitochondrial physiology,
 965 where *specific* refers to the *type of the sample* rather than *mass of the system*. The term
 966 *specific*, therefore, must be clarified; *sample-specific*, *e.g.*, muscle mass-specific
 967 normalization, is distinguished from *system-specific* quantities (mass or volume; Figure 6).
- 968 • **Intensive quantities:** In contrast to size-specific properties, forces are intensive quantities
 969 defined as the change of an extensive quantity per advancement of an energy transformation
 970 (Gnaiger 1993b).
- 971 • N_X and m_X indicate the number format and mass format, respectively, for expressing the
 972 quantity of a sample *X*. When different formats are indicated in symbols of derived quantities,
 973 the format (\underline{N} , \underline{m}) is shown as a subscript (*underlined italic*), as in $I_{O_2/\underline{N}X}$ and $J_{O_2/\underline{m}X}$. Oxygen
 974 flow and flux are expressed in the molar format, n_{O_2} [mol], but in the volume format, V_{O_2} [m³]
 975 in ergometry. For mass-specific flux these formats can be distinguished as $J_{nO_2/\underline{m}X}$ and $J_{VO_2/\underline{m}X}$,
 976 respectively. Further examples are given in Figure 6 and Table 4.

977

978 **Figure 6. Flow and flux, and**
 979 **normalization in structure-**
 980 **function analysis**

981 (A) When expressing metabolic
 982 ‘rate’ measured in a chamber, a
 983 fundamental distinction is made
 984 between relating the rate to the
 985 experimental sample (left) or
 986 chamber (right). The different
 987 meanings of rate need to be
 988 specified by the chosen
 989 normalization. Left: Results are
 990 expressed as mass-specific flux, J_{mX} ,
 991 per mg protein, dry or wet mass.
 992 Cell volume, V_{ce} , may be used for
 993 normalization (volume-specific
 994 flux, J_{Vce}). Right: Flow per chamber,
 995 I , or flux per chamber volume, J_V ,
 996 are merely reported for
 997 methodological reasons.

998 (B) O_2 flow per cell, $I_{O_2/Nce}$, is the
 999 product of mitochondria-specific
 1000 flux, mt-density and mass per cell.
 1001 Unstructured analysis: performance
 1002 is the product of mass-specific flux,
 1003 $J_{O_2/MX}$ [$\text{mol}\cdot\text{s}^{-1}\cdot\text{kg}^{-1}$], and size
 1004 (mass per cell). Structured analysis:
 1005 performance is the product of
 1006 mitochondrial function (mt-specific
 1007 flux) and structure (mt-content).
 1008 Modified from Gnaiger (2014). For
 1009 further details see **Table 4**.



1015 **Box 2: Metabolic flows and fluxes: vectoral, vectorial, and scalar**

1016
 1017 In a generalization of electrical terms, flow as an extensive quantity (I ; per system) is
 1018 distinguished from flux as a size-specific quantity (J ; per system size). *Flows*, I_{tr} , are defined for all
 1019 transformations as extensive quantities. Electric charge per unit time is electric flow or current, $I_{el} =$
 1020 $dQ_{el}\cdot dt^{-1}$ [$A \equiv C\cdot s^{-1}$]. When dividing I_{el} by size of the system (cross-sectional area of a ‘wire’), we obtain
 1021 flux as a size-specific quantity, which is the current density (surface-density of flow) perpendicular to
 1022 the direction of flux, $J_{el} = I_{el}\cdot A^{-1}$ [$A\cdot m^{-2}$] (Cohen et al. 2008). Fluxes with *spatial* geometric direction and
 1023 magnitude are *vectors*. Vector and scalar *fluxes* are related to flows as $J_{tr} = I_{tr}\cdot A^{-1}$ [$\text{mol}\cdot\text{s}^{-1}\cdot\text{m}^{-2}$] and $J_{tr} =$
 1024 $I_{tr}\cdot V^{-1}$ [$\text{mol}\cdot\text{s}^{-1}\cdot\text{m}^{-3}$], expressing flux as an area-specific vector or volume-specific vectorial or scalar
 1025 quantity, respectively (Gnaiger 1993b). We use the metre–kilogram–second–ampere (MKSA)
 1026 international system of units (SI) for general cases ([m], [kg], [s] and [A]), with decimal SI prefixes for
 1027 specific applications (**Table 4**).

1028 We suggest defining: (1) *vectoral* fluxes, which are translocations as functions of *gradients* with
 1029 direction in geometric space in continuous systems; (2) *vectorial* fluxes, which describe translocations
 1030 in discontinuous systems and are restricted to information on *compartmental differences*
 1031 (transmembrane proton flux); and (3) *scalar* fluxes, which are transformations in a *homogenous* system
 1032 (catabolic O_2 flux, J_{kO_2}).

4. Normalization of rate per sample

The challenges of measuring mitochondrial respiratory flux are matched by those of normalization. Normalization (**Table 4**) is guided by physicochemical principles, methodological considerations, and conceptual strategies (**Figure 6**).

Table 4. Sample concentrations and normalization of flux.

Expression	Symbol	Definition	Unit	Notes
Sample				
identity of sample	X	object: cell, tissue, animal, patient		
number of sample entities X	N_X	number of objects	x	1
mass of sample X	m_X		kg	2
mass of object X	M_X	$M_X = m_X \cdot N_X^{-1}$	$\text{kg} \cdot \text{x}^{-1}$	2
Mitochondria				
mitochondria	mt	$X = \text{mt}$		
amount of mt-elementary components	mtE	quantity of mt-marker	mtEU	
Concentrations				
object number concentration	C_{NX}	$C_{NX} = N_X \cdot V^{-1}$	$\text{x} \cdot \text{m}^{-3}$	3
sample mass concentration	C_{mX}	$C_{mX} = m_X \cdot V^{-1}$	$\text{kg} \cdot \text{m}^{-3}$	
mitochondrial concentration	C_{mtE}	$C_{mtE} = mtE \cdot V^{-1}$	$\text{mtEU} \cdot \text{m}^{-3}$	4
specific mitochondrial density	D_{mtE}	$D_{mtE} = mtE \cdot m_X^{-1}$	$\text{mtEU} \cdot \text{kg}^{-1}$	5
mitochondrial content, mtE per object X	mtE_{NX}	$mtE_{NX} = mtE \cdot N_X^{-1}$	$\text{mtEU} \cdot \text{x}^{-1}$	6
O₂ flow and flux				
flow, system	I_{O_2}	internal flow	$\text{mol} \cdot \text{s}^{-1}$	7
volume-specific flux	J_{V,O_2}	$J_{V,O_2} = I_{O_2} \cdot V^{-1}$	$\text{mol} \cdot \text{s}^{-1} \cdot \text{m}^{-3}$	8
flow per object X	$I_{O_2/NX}$	$I_{O_2/NX} = J_{V,O_2} \cdot C_{NX}^{-1}$	$\text{mol} \cdot \text{s}^{-1} \cdot \text{x}^{-1}$	9
mass-specific flux	$J_{O_2/mX}$	$J_{O_2/mX} = J_{V,O_2} \cdot C_{mX}^{-1}$	$\text{mol} \cdot \text{s}^{-1} \cdot \text{kg}^{-1}$	10
mt-marker-specific flux	$J_{O_2/mtE}$	$J_{O_2/mtE} = J_{V,O_2} \cdot C_{mtE}^{-1}$	$\text{mol} \cdot \text{s}^{-1} \cdot \text{mtEU}^{-1}$	11

- 1041 1 The unit x for a number is not used by IUPAC. To avoid confusion, the units [$\text{kg} \cdot \text{x}^{-1}$] and [kg] distinguish the mass per object from the mass of a sample that may contain any number of objects. Similarly, the units for flow per system *versus* flow per object are [$\text{mol} \cdot \text{s}^{-1}$] (Note 8) and [$\text{mol} \cdot \text{s}^{-1} \cdot \text{x}^{-1}$] (Note 10).
- 1042 2 Units are given in the MKSA system (**Box 2**). The SI prefix k is used for the SI base unit of mass (kg = 1,000 g). In praxis, various SI prefixes are used for convenience, to make numbers easily readable, e.g., 1 mg tissue, cell or mitochondrial mass instead of 0.000001 kg.
- 1043 3 In case of cells (sample $X = \text{cells}$), the object number concentration is $C_{N_{ce}} = N_{ce} \cdot V^{-1}$, and volume may be expressed in [$\text{dm}^3 \equiv \text{L}$] or [$\text{cm}^3 = \text{mL}$]. See **Table 5** for different object types.
- 1044 4 mt-concentration is an experimental variable, dependent on sample concentration: (1) $C_{mtE} = mtE \cdot V^{-1}$; (2) $C_{mtE} = mtE_X \cdot C_{NX}$; (3) $C_{mtE} = C_{mX} \cdot D_{mtE}$.
- 1045 5 If the amount of mitochondria, mtE , is expressed as mitochondrial mass, then D_{mtE} is the mass fraction of mitochondria in the sample. If mtE is expressed as mitochondrial volume, V_{mt} , and the mass of sample, m_X , is replaced by volume of sample, V_X , then D_{mtE} is the volume fraction of mitochondria in the sample.
- 1046 6 $mtE_{NX} = mtE \cdot N_X^{-1} = C_{mtE} \cdot C_{NX}^{-1}$.
- 1047 7 O₂ can be replaced by other chemicals to study different reactions, e.g., ATP, H₂O₂, or vesicular compartmental translocations, e.g., Ca²⁺.

- 1059 8 I_{O_2} and V are defined per instrument chamber as a system of constant volume (and constant
 1060 temperature), which may be closed or open. I_{O_2} is abbreviated for I_{rO_2} , *i.e.*, the metabolic or internal
 1061 O_2 flow of the chemical reaction r in which O_2 is consumed, hence the negative stoichiometric
 1062 number, $\nu_{O_2} = -1$. $I_{rO_2} = d_r n_{O_2} / dt \cdot \nu_{O_2}^{-1}$. If r includes all chemical reactions in which O_2 participates, then
 1063 $d_r n_{O_2} = dn_{O_2} - d_e n_{O_2}$, where dn_{O_2} is the change in the amount of O_2 in the instrument chamber and $d_e n_{O_2}$
 1064 is the amount of O_2 added externally to the system. At steady state, by definition $dn_{O_2} = 0$, hence $d_r n_{O_2}$
 1065 $= -d_e n_{O_2}$. Note that in this context ‘external’, e , refers to the system, whereas in Figure 1 ‘external’,
 1066 ext , refers to the organism.
 1067 9 J_{V,O_2} is an experimental variable, expressed per volume of the instrument chamber.
 1068 10 $I_{O_2/NX}$ is a physiological variable, depending on the size of entity X .
 1069 11 There are many ways to normalize for a mitochondrial marker, that are used in different experimental
 1070 approaches: (1) $J_{O_2/mtE} = J_{V,O_2} \cdot C_{mtE}^{-1}$; (2) $J_{O_2/mtE} = J_{V,O_2} \cdot C_{mX}^{-1} \cdot D_{mtE}^{-1} = J_{O_2/mX} \cdot D_{mtE}^{-1}$; (3) $J_{O_2/mtE} =$
 1071 $J_{V,O_2} \cdot C_{NX}^{-1} \cdot mtE_{NX}^{-1} = I_{O_2/NX} \cdot mtE_{NX}^{-1}$; (4) $J_{O_2/mtE} = I_{O_2} \cdot mtE^{-1}$. The mt-elementary unit [mtEU] varies depending
 1072 on the mt-marker.
 1073
 1074
 1075

Table 5. Sample types, X, abbreviations, and quantification.

Identity of sample	X	N_X	Mass ^a	Volume	mt-Marker
mitochondrial preparation		[x]	[kg]	[m ³]	[mtEU]
isolated mitochondria	imt		m_{mt}	V_{mt}	mtE
tissue homogenate	thom		m_{thom}		mtE_{thom}
permeabilized tissue	pti		m_{pti}		mtE_{pti}
permeabilized fibre	pfi		m_{pfi}		mtE_{pfi}
permeabilized cell	pce	N_{pce}	M_{pce}	V_{pce}	mtE_{pce}
cells ^b	ce	N_{ce}	M_{ce}	V_{ce}	mtE_{ce}
intact cell, viable cell	vce	N_{vce}	M_{vce}	V_{vce}	
dead cell	dce	N_{dce}	M_{dce}	V_{dce}	
organism	org	N_{org}	M_{org}	V_{org}	

^a Instead of mass, the wet weight or dry weight is frequently stated, W_w or W_d . m_X is mass of the sample [kg], M_X is mass of the object [kg·x⁻¹] (Table 4).

^b Total cell count, $N_{ce} = N_{vce} + N_{dce}$

4.1. Flow: per object

4.1.1. Number concentration, C_{NX} : Normalization per sample concentration is routinely required to report respiratory data. C_{NX} is the experimental number concentration of sample X . In the case of animals, *e.g.*, nematodes, $C_{NX} = N_X/V$ [x·L⁻¹], where N_X is the number of organisms in the chamber. Similarly, the number of cells per chamber volume is the number concentration of permeabilized or intact cells $C_{Nce} = N_{ce}/V$ [x·L⁻¹], where N_{ce} is the number of cells in the chamber (Table 4).

4.1.2. Flow per object, $I_{O_2/NX}$: O_2 flow per cell is calculated from volume-specific O_2 flux, J_{V,O_2} [nmol·s⁻¹·L⁻¹] (per V of the measurement chamber [L]), divided by the number concentration of cells. The total cell count is the sum of viable and dead cells, $N_{ce} = N_{vce} + N_{dce}$ (Table 5). The cell viability index, $VI = N_{vce}/N_{ce}$, is the ratio of viable cells (N_{vce} ; before experimental permeabilization) per total cell count. After experimental permeabilization, all cells are permeabilized, $N_{pce} = N_{ce}$. The cell viability index can be used to normalize respiration for the number of cells that have been viable before experimental permeabilization, $I_{O_2/Nvce} = I_{O_2/Nce}/VI$, considering that mitochondrial respiratory dysfunction in dead cells should be eliminated as a confounding factor.

The complexity changes when the object is a whole organism studied as an experimental model. The scaling law in respiratory physiology reveals a strong interaction between O_2 flow and individual body mass: *basal* metabolic rate (flow) does not increase linearly with body mass, whereas *maximum* mass-specific O_2 flux, \dot{V}_{O_2max} or \dot{V}_{O_2peak} , is approximately constant across a large range of individual body mass (Weibel and Hoppeler 2005). Individuals, breeds and species, however, deviate substantially from this relationship. \dot{V}_{O_2peak} of human endurance athletes is 60 to 80 mL $O_2 \cdot \text{min}^{-1} \cdot \text{kg}^{-1}$ body mass, converted to $J_{O_2peak/Morg}$ of 45 to 60 nmol·s⁻¹·g⁻¹ (Gnaiger 2014; Table 6).

4.2. Size-specific flux: per sample size

4.2.1. Sample concentration, C_{mX} : Considering permeabilized tissue, homogenate or cells as the sample, X , the sample mass is m_X [mg], which is frequently measured as wet or dry weight, W_w or W_d [mg], respectively, or as amount of protein, m_{Protein} . The sample concentration is the mass of the subsample per volume of the measurement chamber, $C_{mX} = m_X/V$ [$\text{g}\cdot\text{L}^{-1} = \text{mg}\cdot\text{mL}^{-1}$]. X is the type of sample—isolated mitochondria, tissue homogenate, permeabilized fibres or cells (**Table 5**).

4.2.2. Size-specific flux: Cellular O_2 flow can be compared between cells of identical size. To take into account changes and differences in cell size, normalization is required to obtain cell size-specific or mitochondrial marker-specific O_2 flux (Renner *et al.* 2003).

- **Mass-specific flux, $J_{\text{O}_2/mX}$ [$\text{mol}\cdot\text{s}^{-1}\cdot\text{kg}^{-1}$]:** Mass-specific flux is obtained by expressing respiration per mass of sample, m_X [mg]. Flow per cell is divided by mass per cell, $J_{\text{O}_2/mce} = I_{\text{O}_2/Nce}/M_{Nce}$. Or chamber volume-specific flux, J_{V,O_2} , is divided by mass concentration of X in the chamber, $J_{\text{O}_2/mX} = J_{V,\text{O}_2}/C_{mX}$.
- **Cell volume-specific flux, $J_{\text{O}_2/VX}$ [$\text{mol}\cdot\text{s}^{-1}\cdot\text{m}^{-3}$]:** Sample volume-specific flux is obtained by expressing respiration per volume of sample. For example, in the case of using cells as sample will be the volume of cells added to the chamber (**Figure 6**).

If size-specific O_2 flux is constant and independent of sample size, then there is no interaction between the subsystems. For example, a 1.5 mg and a 3.0 mg muscle sample respire at identical mass-specific flux. Mass-specific O_2 flux, however, may change with the mass of a tissue sample, cells or isolated mitochondria in the measuring chamber, in which the nature of the interaction becomes an issue. Therefore, cell density must be optimized, particularly in experiments carried out in wells, considering the confluency of the cell monolayer or clumps of cells (Salabei *et al.* 2014).

4.3. Marker-specific flux: per mitochondrial content

Tissues can contain multiple cell populations that may have distinct mitochondrial subtypes. Mitochondria undergo dynamic fission and fusion cycles, and can exist in multiple stages and sizes that may be altered by a range of factors. The isolation of mitochondria (often achieved through differential centrifugation) can therefore yield a subsample of the mitochondrial types present in a tissue, depending on the isolation protocols utilized, *e.g.*, centrifugation speed. This possible bias should be taken into account when planning experiments using isolated mitochondria. Different sizes of mitochondria are enriched at specific centrifugation speeds, which can be used strategically for isolation of mitochondrial subpopulations.

Part of the mitochondrial content of a tissue is lost during preparation of isolated mitochondria. The fraction of isolated mitochondria obtained from a tissue sample is expressed as mitochondrial recovery. At a high mitochondrial recovery, the fraction of isolated mitochondria is more representative of the total mitochondrial population than in preparations characterized by low recovery. Determination of the mitochondrial recovery and yield is based on measurement of the concentration of a mitochondrial marker in the stock of isolated mitochondria, $C_{mtE,\text{stock}}$, and crude tissue homogenate, $C_{mtE,\text{thom}}$, which simultaneously provides information on the specific mitochondrial density in the sample, D_{mtE} (**Table 4**).

When discussing concepts of normalization, it is essential to consider the question posed by the study. If the study aims at comparing tissue performance—such as the effects of a treatment on a specific tissue, then normalization for tissue mass or protein content is appropriate. However, if the aim is to find differences in mitochondrial function independent of mitochondrial density (**Table 4**), then normalization to a mitochondrial marker is imperative (**Figure 6**). One cannot assume that quantitative changes in various markers—such as mitochondrial proteins—necessarily occur in parallel with one another. It should be established that the marker chosen is not selectively altered by the performed treatment. In conclusion, the normalization must reflect the question under investigation to reach a satisfying answer. On the other hand, the goal of comparing results across projects and institutions requires standardization on normalization for entry into a databank.

4.3.1. Mitochondrial concentration, C_{mtE} , and mitochondrial markers: Mitochondrial organelles compose a dynamic cellular reticulum in various states of fusion and fission. Hence, the definition of an ‘amount’ of mitochondria is often misconceived: mitochondria cannot be counted reliably as a number of occurring elementary components. Therefore, quantification of the amount of

1158 mitochondria depends on the measurement of chosen mitochondrial markers. “Mitochondria are the
 1159 structural and functional elementary units of cell respiration” (Gnaiger 2014). The quantity of a
 1160 mitochondrial marker can reflect the amount of *mitochondrial elementary components*, mtE , expressed
 1161 in various mitochondrial elementary units [mtEU] specific for each measured mt-marker (**Table 4**).
 1162 However, since mitochondrial quality may change in response to stimuli—particularly in mitochondrial
 1163 dysfunction (Campos *et al.* 2017) and after exercise training (Pesta *et al.* 2011) and during aging (Daum
 1164 *et al.* 2013)—some markers can vary while others are unchanged: (1) Mitochondrial volume and
 1165 membrane area are structural markers, whereas mitochondrial protein mass is commonly used as a
 1166 marker for isolated mitochondria. (2) Molecular and enzymatic mitochondrial markers (amounts or
 1167 activities) can be selected as matrix markers, *e.g.*, citrate synthase activity, mtDNA; mtIM-markers, *e.g.*,
 1168 cytochrome *c* oxidase activity, aa_3 content, cardiolipin, or mtOM-markers, *e.g.*, the voltage-dependent
 1169 anion channel (VDAC), TOM20. (3) Extending the measurement of mitochondrial marker enzyme
 1170 activity to mitochondrial pathway capacity, ET- or OXPHOS-capacity can be considered as an
 1171 integrative functional mitochondrial marker.

1172 Depending on the type of mitochondrial marker, the mitochondrial elementary component, mtE ,
 1173 is expressed in marker-specific units. Mitochondrial concentration in the measurement chamber and the
 1174 tissue of origin are quantified as (1) a quantity for normalization in functional analyses, C_{mtE} , and (2) a
 1175 physiological output that is the result of mitochondrial biogenesis and degradation, D_{mtE} , respectively
 1176 (**Table 4**). It is recommended, therefore, to distinguish *experimental mitochondrial concentration*, C_{mtE}
 1177 $= mtE/V$ and *physiological mitochondrial density*, $D_{mtE} = mtE/m_X$. Then mitochondrial density is the
 1178 amount of mitochondrial elementary components per mass of tissue, which is a biological variable
 1179 (**Figure 6**). The experimental variable is mitochondrial density multiplied by sample mass concentration
 1180 in the measuring chamber, $C_{mtE} = D_{mtE} \cdot C_{mX}$, or mitochondrial content multiplied by sample number
 1181 concentration, $C_{mtE} = mtE_X \cdot C_{NX}$ (**Table 4**).

1182 **4.3.2. mt-Marker-specific flux, $J_{O_2/mtE}$:** Volume-specific metabolic O_2 flux depends on: (1) the
 1183 sample concentration in the volume of the instrument chamber, C_{mX} , or C_{NX} ; (2) the mitochondrial
 1184 density in the sample, $D_{mtE} = mtE/m_X$ or $mtE_X = mtE/N_X$; and (3) the specific mitochondrial activity or
 1185 performance per elementary mitochondrial unit, $J_{O_2/mtE} = J_{V,O_2}/C_{mtE}$ [$\text{mol} \cdot \text{s}^{-1} \cdot \text{mtEU}^{-1}$] (**Table 4**).
 1186 Obviously, the numerical results for $J_{O_2/mtE}$ vary with the type of mitochondrial marker chosen for
 1187 measurement of mtE and $C_{mtE} = mtE/V$ [$\text{mtEU} \cdot \text{m}^{-3}$].

1188 Different methods are involved in the quantification of mitochondrial markers and have different
 1189 strengths. Some problems are common for all mitochondrial markers, mtE : (1) Accuracy of
 1190 measurement is crucial, since even a highly accurate and reproducible measurement of O_2 flux results
 1191 in an inaccurate and noisy expression if normalized by a biased and noisy measurement of a
 1192 mitochondrial marker. This problem is acute in mitochondrial respiration because the denominators used
 1193 (the mitochondrial markers) are often small moieties of which accurate and precise determination is
 1194 difficult. This problem can be avoided when O_2 fluxes measured in substrate-uncoupler-inhibitor
 1195 titration protocols are normalized for flux in a defined respiratory reference state, which is used as an
 1196 *internal* marker and yields flux control ratios, *FCRs*. *FCRs* are independent of externally measured
 1197 markers and, therefore, are statistically robust, considering the limitations of ratios in general (Jasienski
 1198 and Bazzaz 1999). *FCRs* indicate qualitative changes of mitochondrial respiratory control, with highest
 1199 quantitative resolution, separating the effect of mitochondrial density or concentration on $J_{O_2/mX}$ and
 1200 $I_{O_2/NX}$ from that of function per elementary mitochondrial marker, $J_{O_2/mtE}$ (Pesta *et al.* 2011; Gnaiger
 1201 2014). (2) If mitochondrial quality does not change and only the amount of mitochondria varies as a
 1202 determinant of mass-specific flux, any marker is equally qualified in principle; then in practice selection
 1203 of the optimum marker depends only on the accuracy and precision of measurement of the mitochondrial
 1204 marker. (3) If mitochondrial flux control ratios change, then there may not be any best mitochondrial
 1205 marker. In general, measurement of multiple mitochondrial markers enables a comparison and
 1206 evaluation of normalization for these mitochondrial markers. Particularly during postnatal development,
 1207 the activity of marker enzymes—such as cytochrome *c* oxidase and citrate synthase—follows different
 1208 time courses (Drahota *et al.* 2004). Evaluation of mitochondrial markers in healthy controls is
 1209 insufficient for providing guidelines for application in the diagnosis of pathological states and specific
 1210 treatments.

1211 In line with the concept of the respiratory control ratio (Chance and Williams 1955a), the most
 1212 readily used normalization is that of flux control ratios and flux control factors (Gnaiger 2014). Selection
 1213 of the state of maximum flux in a protocol as the reference state has the advantages of: (1) internal

1214 normalization; (2) statistically validated linearization of the response in the range of 0 to 1; and (3)
 1215 consideration of maximum flux for integrating a large number of elementary steps in the OXPHOS- or
 1216 ET-pathways. This reduces the risk of selecting a functional marker that is specifically altered by the
 1217 treatment or pathology, yet increases the chance that the highly integrative pathway is disproportionately
 1218 affected, *e.g.*, the OXPHOS- rather than ET-pathway in case of an enzymatic defect in the
 1219 phosphorylation-pathway. In this case, additional information can be obtained by reporting flux control
 1220 ratios based on a reference state that indicates stable tissue-mass specific flux.

1221 Stereological determination of mitochondrial content via two-dimensional transmission electron
 1222 microscopy can have limitations due to the dynamics of mitochondrial size (Meinild Lundby *et al.*
 1223 2017). Accurate determination of three-dimensional volume by two-dimensional microscopy can be
 1224 both time consuming and statistically challenging (Larsen *et al.* 2012).

1225 The validity of using mitochondrial marker enzymes (citrate synthase activity, CI to CIV amount
 1226 or activity) for normalization of flux is limited in part by the same factors that apply to flux control
 1227 ratios. Strong correlations between various mitochondrial markers and citrate synthase activity
 1228 (Reichmann *et al.* 1985; Boushel *et al.* 2007; Mogensen *et al.* 2007) are expected in a specific tissue of
 1229 healthy persons and in disease states not specifically targeting citrate synthase. Citrate synthase activity
 1230 is acutely modifiable by exercise (Tonkonogi *et al.* 1997; Leek *et al.* 2001). Evaluation of mitochondrial
 1231 markers related to a selected age and sex cohort cannot be extrapolated to provide recommendations for
 1232 normalization in respirometric diagnosis of disease, in different states of development and ageing,
 1233 different cell types, tissues, and species. mtDNA normalized to nDNA via qPCR is correlated to
 1234 functional mitochondrial markers including OXPHOS- and ET-capacity in some cases (Puntschart *et al.*
 1235 1995; Wang *et al.* 1999; Menshikova *et al.* 2006; Boushel *et al.* 2007; Ehinger *et al.* 2015), but lack of
 1236 such correlations have been reported (Menshikova *et al.* 2005; Schultz and Wiesner 2000; Pesta *et al.*
 1237 2011). Several studies indicate a strong correlation between cardiolipin content and increase in
 1238 mitochondrial function with exercise (Menshikova *et al.* 2005; Menshikova *et al.* 2007; Larsen *et al.*
 1239 2012; Faber *et al.* 2014), but it has not been evaluated as a general mitochondrial biomarker in disease.
 1240 With no single best mitochondrial marker, a good strategy is to quantify several different biomarkers to
 1241 minimize the decorrelating effects caused by diseases, treatments, or other factors. Determination of
 1242 multiple markers, particularly a matrix marker and a marker from the mtIM, allows tracking changes in
 1243 mitochondrial quality defined by their ratio.

1244
 1245

1246 5. Normalization of rate per system

1247

1248 5.1. Flow: per chamber

1249

1250 The experimental system (experimental chamber) is part of the measurement instrument,
 1251 separated from the environment as an isolated, closed, open, isothermal or non-isothermal system
 1252 (Table 4). Reporting O₂ flows per respiratory chamber, I_{O_2} [nmol·s⁻¹], restricts the analysis to intra-
 1253 experimental comparison of relative differences.

1254

1255 5.2. Flux: per chamber volume

1256

1257 **5.2.1. System-specific flux, J_{V,O_2} :** We distinguish between (1) the *system* with volume V and mass
 1258 m defined by the system boundaries, and (2) the *sample* or *objects* with volume V_X and mass m_X that are
 1259 enclosed in the experimental chamber (Figure 6). Metabolic O₂ flow per object, I_{O_2/N_X} , is the total O₂
 1260 flow in the system divided by the number of objects, N_X , in the system. I_{O_2/N_X} increases as the mass of
 1261 the object is increased. Sample mass-specific O₂ flux, J_{O_2/m_X} should be independent of the mass of the
 1262 sample studied in the instrument chamber, but system volume-specific O₂ flux, J_{V,O_2} (per volume of the
 1263 instrument chamber), increases in proportion to the mass of the sample in the chamber. Although J_{V,O_2}
 1264 depends on mass-concentration of the sample in the chamber, it should be independent of the chamber
 1265 (system) volume at constant sample mass-concentration. There are practical limitations to increasing the
 1266 mass-concentration of the sample in the chamber, when one is concerned about crowding effects and
 1267 instrumental time resolution.

1268

1269 **5.2.2. Advancement per volume:** When the reactor volume does not change during the reaction,
 which is typical for liquid phase reactions, the volume-specific flux of a chemical reaction r is the time

1270 derivative of the advancement of the reaction per unit volume, $J_{V,rB} = d_r \zeta_B / dt \cdot V^{-1}$ [(mol·s⁻¹)·L⁻¹]. The *rate*
 1271 *of concentration change* is dc_B/dt [(mol·L⁻¹)·s⁻¹], where concentration is $c_B = n_B/V$. There is a difference
 1272 between (1) J_{V,rO_2} [mol·s⁻¹·L⁻¹] and (2) rate of concentration change [mol·L⁻¹·s⁻¹]. These merge into a
 1273 single expression only in closed systems. In open systems, internal transformations (catabolic flux, O₂
 1274 consumption) are distinguished from external flux (such as O₂ supply). External fluxes of all substances
 1275 are zero in closed systems. In a closed chamber O₂ consumption (internal flux of catabolic reactions k ;
 1276 I_{kO_2} [pmol·s⁻¹]) causes a decline in the amount of O₂ in the system, n_{O_2} [nmol]. Normalization of these
 1277 quantities for the volume of the system, V [L \equiv dm³], yields volume-specific O₂ flux, $J_{V,kO_2} = I_{kO_2}/V$
 1278 [nmol·s⁻¹·L⁻¹], and O₂ concentration, [O₂] or $c_{O_2} = n_{O_2}/V$ [μ mol·L⁻¹ = μ M = nmol·mL⁻¹]. Instrumental
 1279 background O₂ flux is due to external flux into a non-ideal closed respirometer, so total volume-specific
 1280 flux has to be corrected for instrumental background O₂ flux—O₂ diffusion into or out of the
 1281 instrumental chamber. J_{V,kO_2} is relevant mainly for methodological reasons and should be compared with
 1282 the accuracy of instrumental resolution of background-corrected flux, *e.g.*, ± 1 nmol·s⁻¹·L⁻¹ (Gnaiger
 1283 2001). ‘Catabolic’ indicates O₂ flux, J_{kO_2} , corrected for: (1) instrumental background O₂ flux; (2)
 1284 chemical background O₂ flux due to autoxidation of chemical components added to the incubation
 1285 medium; and (3) *Rox* for O₂-consuming side reactions unrelated to the catabolic pathway k .

1286
1287

1288 6. Conversion of units

1289

1290 Many different units have been used to report the O₂ consumption rate, OCR (Table 6). SI base
 1291 units provide the common reference to introduce the theoretical principles (Figure 6), and are used with
 1292 appropriately chosen SI prefixes to express numerical data in the most practical format, with an effort
 1293 towards unification within specific areas of application (Table 7). Reporting data in SI units—including
 1294 the mole [mol], coulomb [C], joule [J], and second [s]—should be encouraged, particularly by journals
 1295 that propose the use of SI units.

1296

1297 **Table 6. Conversion of various formats and units used in respirometry and**
 1298 **ergometry.** e^- is the number of electrons or reducing equivalents. z_B is the charge number
 1299 of entity B.

1300

Format	1 Unit		Multiplication factor	SI-unit	Notes
\underline{n}	ng.atom O·s ⁻¹	(2 e^-)	0.5	nmol O ₂ ·s ⁻¹	
\underline{n}	ng.atom O·min ⁻¹	(2 e^-)	8.33	pmol O ₂ ·s ⁻¹	
\underline{n}	natom O·min ⁻¹	(2 e^-)	8.33	pmol O ₂ ·s ⁻¹	
\underline{n}	nmol O ₂ ·min ⁻¹	(4 e^-)	16.67	pmol O ₂ ·s ⁻¹	
\underline{n}	nmol O ₂ ·h ⁻¹	(4 e^-)	0.2778	pmol O ₂ ·s ⁻¹	
\underline{V} to \underline{n}	mL O ₂ ·min ⁻¹ at STPD ^a		0.744	μ mol O ₂ ·s ⁻¹	1
\underline{e} to \underline{n}	W = J/s at -470 kJ/mol O ₂		-2.128	μ mol O ₂ ·s ⁻¹	
\underline{e} to \underline{n}	mA = mC·s ⁻¹	($z_{H^+} = 1$)	10.36	nmol H ⁺ ·s ⁻¹	2
\underline{e} to \underline{n}	mA = mC·s ⁻¹	($z_{O_2} = 4$)	2.59	nmol O ₂ ·s ⁻¹	2
\underline{n} to \underline{e}	nmol H ⁺ ·s ⁻¹	($z_{H^+} = 1$)	0.09649	mA	3
\underline{n} to \underline{e}	nmol O ₂ ·s ⁻¹	($z_{O_2} = 4$)	0.38594	mA	3

1301 1 At standard temperature and pressure dry (STPD: 0 °C = 273.15 K and 1 atm = 101.325 kPa =
 1302 760 mmHg), the molar volume of an ideal gas, V_m , and V_{m,O_2} is 22.414 and 22.392 L·mol⁻¹,
 1303 respectively. Rounded to three decimal places, both values yield the conversion factor of 0.744.
 1304 For comparison at normal temperature and pressure dry (NTPD: 20 °C), V_{m,O_2} is 24.038 L·mol⁻¹.
 1305 Note that the SI standard pressure is 100 kPa.

1306 2 The multiplication factor is $10^6/(z_B \cdot F)$.

1307 3 The multiplication factor is $z_B \cdot F/10^6$.

1308

1309 **Table 7. Conversion of units with preservation of numerical values.**

Name	Frequently used unit	Equivalent unit	Notes
volume-specific flux, J_{V,O_2}	$\text{pmol}\cdot\text{s}^{-1}\cdot\text{mL}^{-1}$	$\text{nmol}\cdot\text{s}^{-1}\cdot\text{L}^{-1}$	1
cell-specific flow, $I_{O_2/\text{cell}}$	$\text{mmol}\cdot\text{s}^{-1}\cdot\text{L}^{-1}$	$\text{mol}\cdot\text{s}^{-1}\cdot\text{m}^{-3}$	
	$\text{pmol}\cdot\text{s}^{-1}\cdot 10^{-6}$ cells	$\text{amol}\cdot\text{s}^{-1}\cdot\text{cell}^{-1}$	2
cell number concentration, C_{Nce}	$\text{pmol}\cdot\text{s}^{-1}\cdot 10^{-9}$ cells	$\text{zmol}\cdot\text{s}^{-1}\cdot\text{cell}^{-1}$	3
	10^6 cells $\cdot\text{mL}^{-1}$	10^9 cells $\cdot\text{L}^{-1}$	
mitochondrial protein concentration, C_{mtE}	0.1 mg $\cdot\text{mL}^{-1}$	0.1 g $\cdot\text{L}^{-1}$	
mass-specific flux, $J_{O_2/m}$	$\text{pmol}\cdot\text{s}^{-1}\cdot\text{mg}^{-1}$	$\text{nmol}\cdot\text{s}^{-1}\cdot\text{g}^{-1}$	4
catabolic power, P_k	$\mu\text{W}\cdot 10^{-6}$ cells	$\text{pW}\cdot\text{cell}^{-1}$	1
volume	1,000 L	m^3 (1,000 kg)	
	L	dm^3 (kg)	
	mL	cm^3 (g)	
	μL	mm^3 (mg)	
	fL	μm^3 (pg)	5
amount of substance concentration	$\text{M} = \text{mol}\cdot\text{L}^{-1}$	$\text{mol}\cdot\text{dm}^{-3}$	

1310 1 pmol: picomole = 10^{-12} mol1311 2 amol: attomole = 10^{-18} mol1312 3 zmol: zeptomole = 10^{-21} mol

1313

1314 Although volume is expressed as m^3 using the SI base unit, the litre [dm^3] is a conventional unit
 1315 of volume for concentration and is used for most solution chemical kinetics. If one multiplies $I_{O_2/Nce}$ by
 1316 C_{Nce} , then the result will not only be the amount of O_2 [mol] consumed per time [s^{-1}] in one litre [L^{-1}],
 1317 but also the change in O_2 concentration per second (for any volume of an ideally closed system). This
 1318 is ideal for kinetic modeling as it blends with chemical rate equations where concentrations are typically
 1319 expressed in $\text{mol}\cdot\text{L}^{-1}$ (Wagner *et al.* 2011). In studies of multinuclear cells—such as differentiated
 1320 skeletal muscle cells—it is easy to determine the number of nuclei but not the total number of cells. A
 1321 generalized concept, therefore, is obtained by substituting cells by nuclei as the sample entity. This does
 1322 not hold, however, for non-nucleated platelets.

1323 For studies of cells, we recommend that respiration be expressed, as far as possible, as: (1) O_2
 1324 flux normalized for a mitochondrial marker, for separation of the effects of mitochondrial quality and
 1325 content on cell respiration (this includes $FCRs$ as a normalization for a functional mitochondrial
 1326 marker); (2) O_2 flux in units of cell volume or mass, for comparison of respiration of cells with different
 1327 cell size (Renner *et al.* 2003) and with studies on tissue preparations, and (3) O_2 flow in units of attomole
 1328 (10^{-18} mol) of O_2 consumed per second by each cell [$\text{amol}\cdot\text{s}^{-1}\cdot\text{cell}^{-1}$], numerically equivalent to
 1329 [$\text{pmol}\cdot\text{s}^{-1}\cdot 10^{-6}$ cells]. This convention allows information to be easily used when designing experiments
 1330 in which O_2 flow must be considered. For example, to estimate the volume-specific O_2 flux in an
 1331 instrument chamber that would be expected at a particular cell number concentration, one simply needs
 1332 to multiply the flow per cell by the number of cells per volume of interest. This provides the amount of
 1333 O_2 [mol] consumed per time [s^{-1}] per unit volume [L^{-1}]. At an O_2 flow of 100 $\text{amol}\cdot\text{s}^{-1}\cdot\text{cell}^{-1}$ and a cell
 1334 density of 10^9 cells $\cdot\text{L}^{-1}$ (10^6 cells $\cdot\text{mL}^{-1}$), the volume-specific O_2 flux is 100 $\text{nmol}\cdot\text{s}^{-1}\cdot\text{L}^{-1}$ (100
 1335 $\text{pmol}\cdot\text{s}^{-1}\cdot\text{mL}^{-1}$).

1336 ET-capacity in human cell types including HEK 293, primary HUVEC, and fibroblasts ranges
 1337 from 50 to 180 $\text{amol}\cdot\text{s}^{-1}\cdot\text{cell}^{-1}$, measured in intact cells in the noncoupled state (see Gnaiger 2014). At
 1338 100 $\text{amol}\cdot\text{s}^{-1}\cdot\text{cell}^{-1}$ corrected for Rox , the current across the mt-membranes, I_{H^+e} , approximates 193
 1339 $\text{pA}\cdot\text{cell}^{-1}$ or 0.2 nA per cell. See Rich (2003) for an extension of quantitative bioenergetics from the
 1340 molecular to the human scale, with a transmembrane proton flux equivalent to 520 A in an adult at a
 1341 catabolic power of -110 W. Modelling approaches illustrate the link between protonmotive force and
 1342 currents (Willis *et al.* 2016).

1343 We consider isolated mitochondria as powerhouses and proton pumps as molecular machines to
 1344 relate experimental results to energy metabolism of the intact cell. The cellular P_{\gg/O_2} based on oxidation

of glycogen is increased by the glycolytic (fermentative) substrate-level phosphorylation of 3 P_»/Glyc or 0.5 mol P_» for each mol O₂ consumed in the complete oxidation of a mol glycosyl unit (Glyc). Adding 0.5 to the mitochondrial P_»/O₂ ratio of 5.4 yields a bioenergetic cell physiological P_»/O₂ ratio close to 6. Two NADH equivalents are formed during glycolysis and transported from the cytosol into the mitochondrial matrix, either by the malate-aspartate shuttle or by the glycerophosphate shuttle (**Figure 2A**) resulting in different theoretical yields of ATP generated by mitochondria, the energetic cost of which potentially must be taken into account. Considering also substrate-level phosphorylation in the TCA cycle, this high P_»/O₂ ratio not only reflects proton translocation and OXPHOS studied in isolation, but integrates mitochondrial physiology with energy transformation in the living cell (Gnaiger 1993a).

7. Conclusions

Catabolic cell respiration is the process of exergonic and exothermic energy transformation in which scalar redox reactions are coupled to vectorial ion translocation across a semipermeable membrane, which separates the small volume of a bacterial cell or mitochondrion from the larger volume of its surroundings. The electrochemical exergy can be partially conserved in the phosphorylation of ADP to ATP or in ion pumping, or dissipated in an electrochemical short-circuit. Respiration is thus clearly distinguished from fermentation as the counterpart of cellular core energy metabolism. An O₂ flux balance scheme illustrates the relationships and general definitions (**Figures 1 and 2**).

Box 3: Recommendations for studies with mitochondrial preparations

- Normalization of respiratory rates should be provided as far as possible:
 1. *Biophysical normalization*: on a per cell basis as O₂ flow; this may not be possible when dealing with coenocytic organisms, *e.g.*, filamentous fungi, or tissues without cross-walls separating individual cells, *e.g.*, muscle fibers.
 2. *Cellular normalization*: per g protein; per cell- or tissue-mass as mass-specific O₂ flux; per cell volume as cell volume-specific flux.
 3. *Mitochondrial normalization*: per mitochondrial marker as mt-specific flux.
- With information on cell size and the use of multiple normalizations, maximum potential information is available (Renner *et al.* 2003; Wagner *et al.* 2011; Gnaiger 2014). Reporting flow in a respiratory chamber [nmol·s⁻¹] is discouraged, since it restricts the analysis to intra-experimental comparison of relative (qualitative) differences.
- Catabolic mitochondrial respiration is distinguished from residual O₂ consumption. Fluxes in mitochondrial coupling states should be, as far as possible, corrected for residual O₂ consumption.
- Different mechanisms of uncoupling should be distinguished by defined terms. The tightness of coupling relates to these uncoupling mechanisms, whereas the coupling stoichiometry varies as a function the substrate type involved in ET-pathways with either three or two redox proton pumps operating in series. Separation of tightness of coupling from the pathway-dependent coupling stoichiometry is possible only when the substrate type undergoing oxidation remains the same for respiration in LEAK-, OXPHOS-, and ET-states. In studies of the tightness of coupling, therefore, simple substrate-inhibitor combinations should be applied to exclude a shift in substrate competition that may occur when providing physiological substrate cocktails.
- In studies of isolated mitochondria, the mitochondrial recovery and yield should be reported. Experimental criteria such as transmission electron microscopy for evaluation of purity versus integrity should be considered. Mitochondrial markers—such as citrate synthase activity as an enzymatic matrix marker—provide a link to the tissue of origin on the basis of calculating the mitochondrial recovery, *i.e.*, the fraction of mitochondrial marker obtained from a unit mass of tissue. Total mitochondrial protein is frequently applied as a mitochondrial marker, which is restricted to isolated mitochondria.
- In studies of permeabilized cells, the viability of the cell culture or cell suspension of origin should be reported. Normalization should be evaluated for total cell count or viable cell count.
- Terms and symbols are summarized in **Table 8**. Their use will facilitate transdisciplinary communication and support further development of a consistent theory of bioenergetics and mitochondrial physiology. Technical terms related to and defined with normal words can be used as

1401 index terms in databases, support the creation of ontologies towards semantic information processing
 1402 (MitoPedia), and help in communicating analytical findings as impactful data-driven stories.
 1403 ‘Making data available without making it understandable may be worse than not making it available
 1404 at all’ (National Academies of Sciences, Engineering, and Medicine 2018). Success will depend on
 1405 taking further steps: (1) exhaustive text-mining considering Omics data and functional data; (2)
 1406 network analysis of Omics data with bioinformatics tools; (3) cross-validation with distinct
 1407 bioinformatics approaches; (4) correlation with functional data; (5) guidelines for biological
 1408 validation of network data. This is a call to carefully contribute to FAIR principles (Findable,
 1409 Accessible, Interoperable, Reusable) for the sharing of scientific data.
 1410

1411
 1412 **Table 8. Terms, symbols, and units.**
 1413
 1414

1415 1416	Term	Symbol	Unit	Links and comments
1417	alternative quinol oxidase	AOX		Figure 2B
1418	adenosine monophosphate	AMP		2 ADP ↔ ATP+AMP
1419	adenosine diphosphate	ADP		Table 1, Figures 2 and 5
1420	adenosine triphosphate	ATP		Figures 2 and 5
1421	adenylates	AMP, ADP, ATP		Section 2.5.1
1422	amount of substance B	n_B	[mol]	
1423	ATP yield per O ₂	$Y_{P\gg/O_2}$		P _{gg} /O ₂ ratio measured in any respiratory state
1424				Figures 1 and 3
1425	catabolic reaction	k		Figures 1 and 3
1426	catabolic respiration	J_{kO_2}	<i>varies</i>	Figures 1 and 3
1427	cell number	N_{ce}	[x]	$N_{ce} = N_{vce} + N_{dce}$; Table 5
1428	cell respiration	J_{rO_2}	<i>varies</i>	Figure 1
1429	cell viability index	VI		$VI = N_{vce}/N_{ce} = 1 - N_{dce}/N_{ce}$
1430	charge number of entity B	z_B		Table 6; $z_{O_2} = 4$
1431	Complexes I to IV	CI to CIV		respiratory ET Complexes; Figure 2B
1432				Box 2
1433	concentration of substance B	$c_B = n_B \cdot V^{-1}$; [B]	[mol·m ⁻³]	Section 2.4.1
1434	coupling control state	CCS		non-viable cells, loss of plasma membrane barrier function; Table 5
1435	dead cell number	N_{dce}	[x]	Table 6
1436	electric format	e	[C]	state; Figures 2B and 4
1437	electron transfer system	ETS		Table 1, Figures 2B and 4; State 3u
1438	ET state	ET		Table 1, Figure 4
1439	ET-capacity	E	<i>varies</i>	system-related extensive quantity; Figure 6
1440	flow, for substance B	I_B	[mol·s ⁻¹]	size-specific quantity; Figure 6
1441	flux, for substance B	J_B	<i>varies</i>	Figure 2C
1442	inorganic phosphate	P _i		Figure 2C
1443	inorganic phosphate carrier	PiC		
1444	intact cell number, viable cell number	N_{vce}	[x]	viable cells, intact plasma membrane barrier function; Table 5
1445	LEAK state	LEAK		state; Table 1, Figure 4; compare State 4
1446	LEAK-respiration	L	<i>varies</i>	Table 1; Figure 4
1447	mass format	m	[kg]	Table 4, Figure 6
1448	mass of sample X	m_X	[kg]	Table 4
1449	mass, dry mass	m_d	[kg]	mass of sample X; Figure 6 (frequently called dry weight)
1450	mass, wet mass	m_w	[kg]	mass of sample X; Figure 6 (frequently called wet weight)
1451				
1452				
1453				
1454				
1455				
1456				
1457				
1458				

1459	mass of object X	$M_X = m_X \cdot N_X^{-1}$	$[\text{kg} \cdot \text{x}^{-1}]$	mass of entity X ; Table 4
1460	MITOCARTA			https://www.broadinstitute.org/scientific-community/science/programs/metabolic-disease-program/publications/mitocarta/mitocarta-in-0
1461				
1462				
1463				
1464				
1465	MitoPedia			http://www.bioblast.at/index.php/MitoPedia
1466	mitochondria or mitochondrial	mt		Box 1
1467	mitochondrial DNA	mtDNA		Box 1
1468	mitochondrial concentration	$C_{mtE} = mtE \cdot V^{-1}$	$[\text{mtEU} \cdot \text{m}^{-3}]$	Table 4
1469	mitochondrial content	mtE_X	$[\text{mtEU} \cdot \text{x}^{-1}]$	$mtE_X = mtE \cdot N_X^{-1}$; Table 4
1470	mitochondrial			
1471	elementary component	mtE	$[\text{mtEU}]$	quantity of mt-marker; Table 4
1472	mitochondrial elementary unit	mtEU	<i>varies</i>	specific units for mt-marker; Table 4
1473	mitochondrial inner membrane	mtIM		MIM is widely used; the first M is replaced by mt; Figure 2; Box 1
1474				
1475	mitochondrial outer membrane	mtOM		MOM is widely used; the first M is replaced by mt; Figure 2; Box 1
1476				
1477	mitochondrial recovery	Y_{mtE}		fraction of mtE recovered in sample from the tissue of origin
1478				
1479	mitochondrial yield	$Y_{mtE/m}$		mt-yield per tissues mass; $Y_{mtE/m} = Y_{mtE} \cdot D_{mtE}$
1480				
1481	molar format	\underline{n}	$[\text{mol}]$	Table 6
1482	negative	neg		Figure 4
1483	number concentration of X	C_{NX}	$[\text{x} \cdot \text{m}^{-3}]$	Table 4
1484	number format	\underline{N}	$[\text{x}]$	Table 4, Figure 6
1485	number of entities X	N_X	$[\text{x}]$	Table 4, Figure 6
1486	number of entity B	N_B	$[\text{x}]$	Table 4
1487	oxidative phosphorylation	OXPHOS		state; Table 1, Figure 4
1488	OXPHOS state	OXPHOS		Table 1; State 3 if $[\text{ADP}]$ and $[\text{P}_i]$ are saturating
1489				
1490	OXPHOS-capacity	P	<i>varies</i>	Table 1, Figure 4
1491	oxygen concentration	$c_{\text{O}_2} = n_{\text{O}_2} \cdot V^{-1}$	$[\text{mol} \cdot \text{m}^{-3}]$	$[\text{O}_2]$; Section 3.2
1492	oxygen flux, in reaction r	$J_{r\text{O}_2}$	<i>varies</i>	Figure 1
1493	pathway control state	PCS		Section 2.2
1494	permeabilized cell number	N_{pce}	$[\text{x}]$	experimental permeabilization of plasma membrane; Table 5
1495				
1496	phosphorylation of ADP to ATP	P_{\gg}		Section 2.2
1497	P_{\gg}/O_2 ratio	P_{\gg}/O_2		mechanistic Y_{P_{\gg}/O_2} , calculated from pump stoichiometries; Figure 2B
1498				
1499	positive	pos		Figure 4
1500	proton in the negative compartment	H^+_{neg}		Figure 4
1501	proton in the positive compartment	H^+_{pos}		Figure 4
1502	protonmotive force	pmf	$[\text{V}]$	Figures 1, 2A and 4; Table 1
1503	rate of electron transfer in ET state	E	<i>varies</i>	ET-capacity; Table 1
1504	rate of LEAK-respiration	L	<i>varies</i>	Table 1
1505	rate of oxidative phosphorylation	P	<i>varies</i>	OXPHOS-capacity; Table 1
1506	rate of residual oxygen consumption	R_{ox}		Table 1, Figure 1
1507	residual oxygen consumption	ROX		state; Table 1
1508	respiratory supercomplex	$\text{SC I}_n\text{III}_n\text{IV}_n$		supramolecular assemblies composed of variable copy numbers (n) of CI, CIII and CIV; Box 1
1509				
1510				
1511	specific mitochondrial density	$D_{mtE} = mtE \cdot m_X^{-1}$	$[\text{mtEU} \cdot \text{kg}^{-1}]$	Table 4
1512	substrate-uncoupler-inhibitor-titration protocol	SUIT		Section 2.2
1513				
1514	volume	V	$[\text{m}^{-3}]$	Table 7

1516
1517
1518 Experimentally, respiration is separated in mitochondrial preparations from the interactions with
1519 the fermentative pathways of the intact cell. OXPHOS analysis is based on the study of mitochondrial
1520 preparations complementary to bioenergetic investigations of intact cells and organisms—from model
1521 organisms to the human species including healthy and diseased persons (patients). Different mechanisms
1522 of respiratory uncoupling have to be distinguished (**Figure 3**). Metabolic fluxes measured in defined
1523 coupling and pathway control states (**Figures 5 and 6**) provide insights into the meaning of cellular and
1524 organismic respiration.

1525 The optimal choice for expressing mitochondrial and cell respiration as O₂ flow per biological
1526 sample, and normalization for specific tissue-markers (volume, mass, protein) and mitochondrial
1527 markers (volume, protein, content, mtDNA, activity of marker enzymes, respiratory reference state) is
1528 guided by the scientific question under study. Interpretation of the data depends critically on appropriate
1529 normalization (**Figure 6**).

1530 MitoEAGLE can serve as a gateway to better diagnose mitochondrial respiratory adaptations and
1531 defects linked to genetic variation, age-related health risks, sex-specific mitochondrial performance,
1532 lifestyle with its effects on degenerative diseases, and thermal and chemical environment. The present
1533 recommendations on coupling control states and rates, linked to the concept of the protonmotive force,
1534 are focused on studies using mitochondrial preparations (**Box 3**). These will be extended in a series of
1535 reports on pathway control of mitochondrial respiration, respiratory states in intact cells, and
1536 harmonization of experimental procedures.

1537 1538 **Acknowledgements**

1539 We thank Beno M for management assistance, and Rich PR for valuable discussions. This publication
1540 is based upon work from COST Action CA15203 MitoEAGLE, supported by COST (European
1541 Cooperation in Science and Technology), in cooperation with COST Actions CA16225 EU-
1542 CARDIOPROTECTION and CA17129 CardioRNA, and K-Regio project MitoFit (E.G.).

1543
1544 **Competing financial interests:** E.G. is founder and CEO of Oroboros Instruments, Innsbruck, Austria.
1545

1546 **References**

- 1547
1548 Altmann R (1894) Die Elementarorganismen und ihre Beziehungen zu den Zellen. Zweite vermehrte Auflage.
1549 Verlag Von Veit & Comp, Leipzig:160 pp.
1550 Baggeto LG, Testa-Perussini R (1990) Role of acetoin on the regulation of intermediate metabolism of Ehrlich
1551 ascites tumor mitochondria: its contribution to membrane cholesterol enrichment modifying passive proton
1552 permeability. Arch Biochem Biophys 283:341-8.
1553 Beard DA (2005) A biophysical model of the mitochondrial respiratory system and oxidative phosphorylation.
1554 PLoS Comput Biol 1(4):e36.
1555 Benda C (1898) Weitere Mitteilungen über die Mitochondria. Verh Dtsch Physiol Ges:376-83.
1556 Birkedal R, Laasmaa M, Vendelin M (2014) The location of energetic compartments affects energetic
1557 communication in cardiomyocytes. Front Physiol 5:376.
1558 Blier PU, Dufresne F, Burton RS (2001) Natural selection and the evolution of mtDNA-encoded peptides:
1559 evidence for intergenomic co-adaptation. Trends Genet 17:400-6.
1560 Blier PU, Guderley HE (1993) Mitochondrial activity in rainbow trout red muscle: the effect of temperature on
1561 the ADP-dependence of ATP synthesis. J Exp Biol 176:145-58.
1562 Breton S, Beaupré HD, Stewart DT, Hoeh WR, Blier PU (2007) The unusual system of doubly uniparental
1563 inheritance of mtDNA: isn't one enough? Trends Genet 23:465-74.
1564 Brown GC (1992) Control of respiration and ATP synthesis in mammalian mitochondria and cells. Biochem J
1565 284:1-13.
1566 Burger G, Gray MW, Forget L, Lang BF (2013) Strikingly bacteria-like and gene-rich mitochondrial genomes
1567 throughout jakobid protists. Genome Biol Evol 5:418-38.
1568 Calvo SE, Klauser CR, Mootha VK (2016) MitoCarta2.0: an updated inventory of mammalian mitochondrial
1569 proteins. Nucleic Acids Research 44:D1251-7.
1570 Calvo SE, Julien O, Clauser KR, Shen H, Kamer KJ, Wells JA, Mootha VK (2017) Comparative analysis of
1571 mitochondrial N-termini from mouse, human, and yeast. Mol Cell Proteomics 16:512-23.

- 1572 Campos JC, Queliconi BB, Bozi LHM, Bechara LRG, Dourado PMM, Andres AM, Jannig PR, Gomes KMS,
 1573 Zambelli VO, Rocha-Resende C, Guatimosim S, Brum PC, Mochly-Rosen D, Gottlieb RA, Kowaltowski AJ,
 1574 Ferreira JCB (2017) Exercise reestablishes autophagic flux and mitochondrial quality control in heart failure.
 1575 *Autophagy* 13:1304-317.
- 1576 Canton M, Luvisetto S, Schmehl I, Azzone GF (1995) The nature of mitochondrial respiration and
 1577 discrimination between membrane and pump properties. *Biochem J* 310:477-81.
- 1578 Carrico C, Meyer JG, He W, Gibson BW, Verdin E (2018) The mitochondrial acylome emerges: proteomics,
 1579 regulation by Sirtuins, and metabolic and disease implications. *Cell Metab* 27:497-512.
- 1580 Chan DC (2006) Mitochondria: dynamic organelles in disease, aging, and development. *Cell* 125:1241-52.
- 1581 Chance B, Williams GR (1955a) Respiratory enzymes in oxidative phosphorylation. I. Kinetics of oxygen
 1582 utilization. *J Biol Chem* 217:383-93.
- 1583 Chance B, Williams GR (1955b) Respiratory enzymes in oxidative phosphorylation: III. The steady state. *J Biol*
 1584 *Chem* 217:409-27.
- 1585 Chance B, Williams GR (1955c) Respiratory enzymes in oxidative phosphorylation. IV. The respiratory chain. *J*
 1586 *Biol Chem* 217:429-38.
- 1587 Chance B, Williams GR (1956) The respiratory chain and oxidative phosphorylation. *Adv Enzymol Relat Subj*
 1588 *Biochem* 17:65-134.
- 1589 Chowdhury SK, Djordjevic J, Albensi B, Fernyhough P (2015) Simultaneous evaluation of substrate-dependent
 1590 oxygen consumption rates and mitochondrial membrane potential by TMRM and safranin in cortical
 1591 mitochondria. *Biosci Rep* 36:e00286.
- 1592 Cobb LJ, Lee C, Xiao J, Yen K, Wong RG, Nakamura HK, Mehta HH, Gao Q, Ashur C, Huffman DM, Wan J,
 1593 Muzumdar R, Barzilai N, Cohen P (2016) Naturally occurring mitochondrial-derived peptides are age-
 1594 dependent regulators of apoptosis, insulin sensitivity, and inflammatory markers. *Aging (Albany NY)* 8:796-
 1595 809.
- 1596 Cohen ER, Cvitas T, Frey JG, Holmström B, Kuchitsu K, Marquardt R, Mills I, Pavese F, Quack M, Stohner J,
 1597 Strauss HL, Takami M, Thor HL (2008) Quantities, units and symbols in physical chemistry, IUPAC Green
 1598 Book, 3rd Edition, 2nd Printing, IUPAC & RSC Publishing, Cambridge.
- 1599 Cooper H, Hedges LV, Valentine JC, eds (2009) *The handbook of research synthesis and meta-analysis*. Russell
 1600 Sage Foundation.
- 1601 Coopersmith J (2010) Energy, the subtle concept. The discovery of Feynman's blocks from Leibnitz to Einstein.
 1602 Oxford University Press:400 pp.
- 1603 Cummins J (1998) Mitochondrial DNA in mammalian reproduction. *Rev Reprod* 3:172-82.
- 1604 Dai Q, Shah AA, Garde RV, Yonish BA, Zhang L, Medvitz NA, Miller SE, Hansen EL, Dunn CN, Price TM
 1605 (2013) A truncated progesterone receptor (PR-M) localizes to the mitochondrion and controls cellular
 1606 respiration. *Mol Endocrinol* 27:741-53.
- 1607 Daum B, Walter A, Horst A, Osiewacz HD, Kühlbrandt W (2013) Age-dependent dissociation of ATP synthase
 1608 dimers and loss of inner-membrane cristae in mitochondria. *Proc Natl Acad Sci U S A* 110:15301-6.
- 1609 Divakaruni AS, Brand MD (2011) The regulation and physiology of mitochondrial proton leak. *Physiology*
 1610 (Bethesda) 26:192-205.
- 1611 Doerrier C, Garcia-Souza LF, Krumschnabel G, Wohlfarter Y, Mészáros AT, Gnaiger E (2018) High-Resolution
 1612 FluoRespirometry and OXPHOS protocols for human cells, permeabilized fibres from small biopsies of
 1613 muscle, and isolated mitochondria. *Methods Mol Biol* 1782 (Palmeira CM, Moreno AJ, eds): Mitochondrial
 1614 Bioenergetics, 978-1-4939-7830-4.
- 1615 Doskey CM, van 't Erve TJ, Wagner BA, Buettner GR (2015) Moles of a substance per cell is a highly
 1616 informative dosing metric in cell culture. *PLoS One* 10:e0132572.
- 1617 Drahotová Z, Milerová M, Stieglerová A, Houstek J, Ostádal B (2004) Developmental changes of cytochrome *c*
 1618 oxidase and citrate synthase in rat heart homogenate. *Physiol Res* 53:119-22.
- 1619 Duarte FV, Palmeira CM, Rolo AP (2014) The role of microRNAs in mitochondria: small players acting wide.
 1620 *Genes (Basel)* 5:865-86.
- 1621 Ehinger JK, Morota S, Hansson MJ, Paul G, Elmér E (2015) Mitochondrial dysfunction in blood cells from
 1622 amyotrophic lateral sclerosis patients. *J Neurol* 262:1493-503.
- 1623 Ernster L, Schatz G (1981) Mitochondria: a historical review. *J Cell Biol* 91:227s-55s.
- 1624 Estabrook RW (1967) Mitochondrial respiratory control and the polarographic measurement of ADP:O ratios.
 1625 *Methods Enzymol* 10:41-7.
- 1626 Faber C, Zhu ZJ, Castellino S, Wagner DS, Brown RH, Peterson RA, Gates L, Barton J, Bickett M, Hagerty L,
 1627 Kimbrough C, Sola M, Bailey D, Jordan H, Elangbam CS (2014) Cardiolipin profiles as a potential
 1628 biomarker of mitochondrial health in diet-induced obese mice subjected to exercise, diet-restriction and
 1629 ephedrine treatment. *J Appl Toxicol* 34:1122-9.
- 1630 Feagin JE, Harrell MI, Lee JC, Coe KJ, Sands BH, Cannone JJ, Tami G, Schnare MN, Gutell RR (2012) The
 1631 fragmented mitochondrial ribosomal RNAs of *Plasmodium falciparum*. *PLoS One* 7:e38320.
- 1632 Fell D (1997) *Understanding the control of metabolism*. Portland Press.

- 1633 Forstner H, Gnaiger E (1983) Calculation of equilibrium oxygen concentration. In: Polarographic Oxygen
 1634 Sensors. Aquatic and Physiological Applications. Gnaiger E, Forstner H (eds), Springer, Berlin, Heidelberg,
 1635 New York:321-33.
- 1636 Garlid KD, Beavis AD, Ratkje SK (1989) On the nature of ion leaks in energy-transducing membranes. *Biochim*
 1637 *Biophys Acta* 976:109-20.
- 1638 Garlid KD, Semrad C, Zinchenko V. Does redox slip contribute significantly to mitochondrial respiration? In:
 1639 Schuster S, Rigoulet M, Ouhabi R, Mazat J-P, eds (1993) Modern trends in biothermokinetics. Plenum Press,
 1640 New York, London:287-93.
- 1641 Gerö D, Szabo C (2016) Glucocorticoids suppress mitochondrial oxidant production via upregulation of
 1642 uncoupling protein 2 in hyperglycemic endothelial cells. *PLoS One* 11:e0154813.
- 1643 Gnaiger E. Efficiency and power strategies under hypoxia. Is low efficiency at high glycolytic ATP production a
 1644 paradox? In: Surviving Hypoxia: Mechanisms of Control and Adaptation. Hochachka PW, Lutz PL, Sick T,
 1645 Rosenthal M, Van den Thillart G, eds (1993a) CRC Press, Boca Raton, Ann Arbor, London, Tokyo:77-109.
- 1646 Gnaiger E (1993b) Nonequilibrium thermodynamics of energy transformations. *Pure Appl Chem* 65:1983-2002.
- 1647 Gnaiger E (2001) Bioenergetics at low oxygen: dependence of respiration and phosphorylation on oxygen and
 1648 adenosine diphosphate supply. *Respir Physiol* 128:277-97.
- 1649 Gnaiger E (2009) Capacity of oxidative phosphorylation in human skeletal muscle. New perspectives of
 1650 mitochondrial physiology. *Int J Biochem Cell Biol* 41:1837-45.
- 1651 Gnaiger E (2014) Mitochondrial pathways and respiratory control. An introduction to OXPHOS analysis. 4th ed.
 1652 *Mitochondr Physiol Network* 19.12. Oroboros MiPNet Publications, Innsbruck:80 pp.
- 1653 Gnaiger E, Méndez G, Hand SC (2000) High phosphorylation efficiency and depression of uncoupled respiration
 1654 in mitochondria under hypoxia. *Proc Natl Acad Sci USA* 97:11080-5.
- 1655 Greggio C, Jha P, Kulkarni SS, Lagarrigue S, Broskey NT, Boutant M, Wang X, Conde Alonso S, Ofori E,
 1656 Auwerx J, Cantó C, Amati F (2017) Enhanced respiratory chain supercomplex formation in response to
 1657 exercise in human skeletal muscle. *Cell Metab* 25:301-11.
- 1658 Hinkle PC (2005) P/O ratios of mitochondrial oxidative phosphorylation. *Biochim Biophys Acta* 1706:1-11.
- 1659 Hofstadter DR (1979) Gödel, Escher, Bach: An eternal golden braid. A metaphorical fugue on minds and
 1660 machines in the spirit of Lewis Carroll. Harvester Press:499 pp.
- 1661 Illaste A, Laasmaa M, Peterson P, Vendelin M (2012) Analysis of molecular movement reveals latticelike
 1662 obstructions to diffusion in heart muscle cells. *Biophys J* 102:739-48.
- 1663 Jasienski M, Bazzaz FA (1999) The fallacy of ratios and the testability of models in biology. *Oikos* 84:321-26.
- 1664 Jepihhina N, Beraud N, Sepp M, Birkedal R, Vendelin M (2011) Permeabilized rat cardiomyocyte response
 1665 demonstrates intracellular origin of diffusion obstacles. *Biophys J* 101:2112-21.
- 1666 Karnkowska A, Vacek V, Zubáčová Z, Treitli SC, Petrželková R, Eme L, Novák L, Žárský V, Barlow LD,
 1667 Herman EK, Soukal P, Hroudová M, Doležal P, Stairs CW, Roger AJ, Eliáš M, Dacks JB, Vlček Č, Hampl V
 1668 (2016) A eukaryote without a mitochondrial organelle. *Curr Biol* 26:1274-84.
- 1669 Klepinin A, Ounpuu L, Guzun R, Chekulayev V, Timohhina N, Tepp K, Shevchuk I, Schlattner U, Kaambre T
 1670 (2016) Simple oxygraphic analysis for the presence of adenylate kinase 1 and 2 in normal and tumor cells. *J*
 1671 *Bioenerg Biomembr* 48:531-48.
- 1672 Klingenberg M (2017) UCP1 - A sophisticated energy valve. *Biochimie* 134:19-27.
- 1673 Koit A, Shevchuk I, Ounpuu L, Klepinin A, Chekulayev V, Timohhina N, Tepp K, Puurand M, Truu L, Heck K,
 1674 Valvere V, Guzun R, Kaambre T (2017) Mitochondrial respiration in human colorectal and breast cancer
 1675 clinical material is regulated differently. *Oxid Med Cell Longev* 1372640.
- 1676 Komlódi T, Tretter L (2017) Methylene blue stimulates substrate-level phosphorylation catalysed by succinyl-
 1677 CoA ligase in the citric acid cycle. *Neuropharmacology* 123:287-98.
- 1678 Korn E (1969) Cell membranes: structure and synthesis. *Annu Rev Biochem* 38:263-88.
- 1679 Lai N, M Kummitha C, Rosca MG, Fujioka H, Tandler B, Hoppel CL (2018) Isolation of mitochondrial
 1680 subpopulations from skeletal muscle: optimizing recovery and preserving integrity. *Acta Physiol*
 1681 (Oxf):e13182. doi: 10.1111/apha.13182.
- 1682 Lane N (2005) Power, sex, suicide: mitochondria and the meaning of life. Oxford University Press:354 pp.
- 1683 Larsen S, Nielsen J, Neigaard Nielsen C, Nielsen LB, Wibrand F, Stride N, Schroder HD, Boushel RC, Helge
 1684 JW, Dela F, Hey-Mogensen M (2012) Biomarkers of mitochondrial content in skeletal muscle of healthy
 1685 young human subjects. *J Physiol* 590:3349-60.
- 1686 Lee C, Zeng J, Drew BG, Sallam T, Martin-Montalvo A, Wan J, Kim SJ, Mehta H, Hevener AL, de Cabo R,
 1687 Cohen P (2015) The mitochondrial-derived peptide MOTS-c promotes metabolic homeostasis and reduces
 1688 obesity and insulin resistance. *Cell Metab* 21:443-54.
- 1689 Lee SR, Kim HK, Song IS, Youm J, Dizon LA, Jeong SH, Ko TH, Heo HJ, Ko KS, Rhee BD, Kim N, Han J
 1690 (2013) Glucocorticoids and their receptors: insights into specific roles in mitochondria. *Prog Biophys Mol*
 1691 *Biol* 112:44-54.
- 1692 Leek BT, Mudaliar SR, Henry R, Mathieu-Costello O, Richardson RS (2001) Effect of acute exercise on citrate
 1693 synthase activity in untrained and trained human skeletal muscle. *Am J Physiol Regul Integr Comp Physiol*
 1694 280:R441-7.

- 1695 Lemieux H, Blier PU, Gnaiger E (2017) Remodeling pathway control of mitochondrial respiratory capacity by
 1696 temperature in mouse heart: electron flow through the Q-junction in permeabilized fibers. *Sci Rep* 7:2840.
 1697 Lenaz G, Tioli G, Falasca AI, Genova ML (2017) Respiratory supercomplexes in mitochondria. In: *Mechanisms*
 1698 *of primary energy trasduction in biology*. M Wikstrom (ed) Royal Society of Chemistry Publishing, London,
 1699 UK:296-337.
- 1700 Liu S, Roellig DM, Guo Y, Li N, Frace MA, Tang K, Zhang L, Feng Y, Xiao L (2016) Evolution of mitosome
 1701 metabolism and invasion-related proteins in *Cryptosporidium*. *BMC Genomics* 17:1006.
- 1702 Margulis L (1970) *Origin of eukaryotic cells*. New Haven: Yale University Press.
- 1703 McDonald AE, Vanlerberghe GC, Staples JF (2009) Alternative oxidase in animals: unique characteristics and
 1704 taxonomic distribution. *J Exp Biol* 212:2627-34.
- 1705 Meinild Lundby AK, Jacobs RA, Gehrig S, de Leur J, Hauser M, Bonne TC, Flück D, Dandanell S, Kirk N,
 1706 Kaech A, Ziegler U, Larsen S, Lundby C (2018) Exercise training increases skeletal muscle mitochondrial
 1707 volume density by enlargement of existing mitochondria and not de novo biogenesis. *Acta Physiol* 222,
 1708 e12905.
- 1709 Menshikova EV, Ritov VB, Fairfull L, Ferrell RE, Kelley DE, Goodpaster BH (2006) Effects of exercise on
 1710 mitochondrial content and function in aging human skeletal muscle. *J Gerontol A Biol Sci Med Sci* 61:534-
 1711 40.
- 1712 Menshikova EV, Ritov VB, Ferrell RE, Azuma K, Goodpaster BH, Kelley DE (2007) Characteristics of skeletal
 1713 muscle mitochondrial biogenesis induced by moderate-intensity exercise and weight loss in obesity. *J Appl*
 1714 *Physiol* (1985) 103:21-7.
- 1715 Menshikova EV, Ritov VB, Toledo FG, Ferrell RE, Goodpaster BH, Kelley DE (2005) Effects of weight loss
 1716 and physical activity on skeletal muscle mitochondrial function in obesity. *Am J Physiol Endocrinol Metab*
 1717 288:E818-25.
- 1718 Miller GA (1991) *The science of words*. Scientific American Library New York:276 pp.
- 1719 Mitchell P (1961) Coupling of phosphorylation to electron and hydrogen transfer by a chemi-osmotic type of
 1720 mechanism. *Nature* 191:144-8.
- 1721 Mitchell P (2011) Chemiosmotic coupling in oxidative and photosynthetic phosphorylation. *Biochim Biophys*
 1722 *Acta Bioenergetics* 1807:1507-38.
- 1723 Mogensen M, Sahlin K, Fernström M, Glinthorg D, Vind BF, Beck-Nielsen H, Højlund K (2007) Mitochondrial
 1724 respiration is decreased in skeletal muscle of patients with type 2 diabetes. *Diabetes* 56:1592-9.
- 1725 Mohr PJ, Phillips WD (2015) Dimensionless units in the SI. *Metrologia* 52:40-7.
- 1726 Moreno M, Giacco A, Di Munno C, Goglia F (2017) Direct and rapid effects of 3,5-diiodo-L-thyronine (T2).
 1727 *Mol Cell Endocrinol* 7207:30092-8.
- 1728 Morrow RM, Picard M, Derbeneva O, Leipzig J, McManus MJ, Gouspillou G, Barbat-Artigas S, Dos Santos C,
 1729 Hepple RT, Murdock DG, Wallace DC (2017) Mitochondrial energy deficiency leads to hyperproliferation of
 1730 skeletal muscle mitochondria and enhanced insulin sensitivity. *Proc Natl Acad Sci U S A* 114:2705-10.
- 1731 Murley A, Nunnari J (2016) The emerging network of mitochondria-organelle contacts. *Mol Cell* 61:648-53.
- 1732 National Academies of Sciences, Engineering, and Medicine (2018) *International coordination for science data*
 1733 *infrastructure: Proceedings of a workshop—in brief*. Washington, DC: The National Academies Press. doi:
 1734 <https://doi.org/10.17226/25015>.
- 1735 Oemer G, Lackner L, Muigg K, Krumschnabel G, Watschinger K, Sailer S, Lindner H, Gnaiger E, Wortmann
 1736 SB, Werner ER, Zschocke J, Keller MA (2018) The molecular structural diversity of mitochondrial
 1737 cardiolipins. *Proc Nat Acad Sci U S A* 115:4158-63.
- 1738 Palmfeldt J, Bross P (2017) Proteomics of human mitochondria. *Mitochondrion* 33:2-14.
- 1739 Paradies G, Paradies V, De Benedictis V, Ruggiero FM, Petrosillo G (2014) Functional role of cardiolipin in
 1740 mitochondrial bioenergetics. *Biochim Biophys Acta* 1837:408-17.
- 1741 Pesta D, Gnaiger E (2012) High-Resolution Respirometry. *OXPHOS protocols for human cells and*
 1742 *permeabilized fibres from small biopsies of human muscle*. *Methods Mol Biol* 810:25-58.
- 1743 Pesta D, Hoppel F, Macek C, Messner H, Faulhaber M, Kobel C, Parson W, Burtcher M, Schocke M, Gnaiger
 1744 E (2011) Similar qualitative and quantitative changes of mitochondrial respiration following strength and
 1745 endurance training in normoxia and hypoxia in sedentary humans. *Am J Physiol Regul Integr Comp Physiol*
 1746 301:R1078–87.
- 1747 Price TM, Dai Q (2015) The role of a mitochondrial progesterone receptor (PR-M) in progesterone action.
 1748 *Semin Reprod Med* 33:185-94.
- 1749 Puchowicz MA, Varnes ME, Cohen BH, Friedman NR, Kerr DS, Hoppel CL (2004) Oxidative phosphorylation
 1750 analysis: assessing the integrated functional activity of human skeletal muscle mitochondria – case studies.
 1751 *Mitochondrion* 4:377-85. Puntschart A, Claassen H, Jostarndt K, Hoppeler H, Billeter R (1995) mRNAs of
 1752 enzymes involved in energy metabolism and mtDNA are increased in endurance-trained athletes. *Am J*
 1753 *Physiol* 269:C619-25.
- 1754 Quiros PM, Mottis A, Auwerx J (2016) Mitonuclear communication in homeostasis and stress. *Nat Rev Mol*
 1755 *Cell Biol* 17:213-26.

- 1756 Rackham O, Mercer TR, Filipovska A (2012) The human mitochondrial transcriptome and the RNA-binding
1757 proteins that regulate its expression. *WIREs RNA* 3:675–95.
- 1758 Reichmann H, Hoppeler H, Mathieu-Costello O, von Bergen F, Pette D (1985) Biochemical and ultrastructural
1759 changes of skeletal muscle mitochondria after chronic electrical stimulation in rabbits. *Pflugers Arch* 404:1-
1760 9.
- 1761 Renner K, Amberger A, Konwalinka G, Gnaiger E (2003) Changes of mitochondrial respiration, mitochondrial
1762 content and cell size after induction of apoptosis in leukemia cells. *Biochim Biophys Acta* 1642:115-23.
- 1763 Rice DW, Alverson AJ, Richardson AO, Young GJ, Sanchez-Puerta MV, Munzinger J, Barry K, Boore JL,
1764 Zhang Y, dePamphilis CW, Knox EB, Palmer JD (2016) Horizontal transfer of entire genomes via
1765 mitochondrial fusion in the angiosperm *Amborella*. *Science* 342:1468-73.
- 1766 Rich P (2003) Chemiosmotic coupling: The cost of living. *Nature* 421:583.
- 1767 Rich PR (2013) Chemiosmotic theory. *Encyclopedia Biol Chem* 1:467-72.
- 1768 Roger JA, Munoz-Gomes SA, Kamikawa R (2017) The origin and diversification of mitochondria. *Curr Biol*
1769 27:R1177-92.
- 1770 Rostovtseva TK, Sheldon KL, Hassanzadeh E, Monge C, Saks V, Bezrukov SM, Sackett DL (2008) Tubulin
1771 binding blocks mitochondrial voltage-dependent anion channel and regulates respiration. *Proc Natl Acad Sci*
1772 USA 105:18746-51.
- 1773 Rustin P, Parfait B, Chretien D, Bourgeron T, Djouadi F, Bastin J, Rötig A, Munnich A (1996) Fluxes of
1774 nicotinamide adenine dinucleotides through mitochondrial membranes in human cultured cells. *J Biol Chem*
1775 271:14785-90.
- 1776 Saks VA, Veksler VI, Kuznetsov AV, Kay L, Sikk P, Tiivel T, Tranqui L, Olivares J, Winkler K, Wiedemann F,
1777 Kunz WS (1998) Permeabilised cell and skinned fiber techniques in studies of mitochondrial function in
1778 vivo. *Mol Cell Biochem* 184:81-100.
- 1779 Salabei JK, Gibb AA, Hill BG (2014) Comprehensive measurement of respiratory activity in permeabilized cells
1780 using extracellular flux analysis. *Nat Protoc* 9:421-38.
- 1781 Sazanov LA (2015) A giant molecular proton pump: structure and mechanism of respiratory complex I. *Nat Rev*
1782 *Mol Cell Biol* 16:375-88.
- 1783 Schneider TD (2006) Claude Shannon: biologist. The founder of information theory used biology to formulate
1784 the channel capacity. *IEEE Eng Med Biol Mag* 25:30-3.
- 1785 Schönfeld P, Dymkowska D, Wojtczak L (2009) Acyl-CoA-induced generation of reactive oxygen species in
1786 mitochondrial preparations is due to the presence of peroxisomes. *Free Radic Biol Med* 47:503-9.
- 1787 Schultz J, Wiesner RJ (2000) Proliferation of mitochondria in chronically stimulated rabbit skeletal muscle--
1788 transcription of mitochondrial genes and copy number of mitochondrial DNA. *J Bioenerg Biomembr* 32:627-
1789 34.
- 1790 Speijer D (2016) Being right on Q: shaping eukaryotic evolution. *Biochem J* 473:4103-27.
- 1791 Sugiura A, Mattie S, Prudent J, McBride HM (2017) Newly born peroxisomes are a hybrid of mitochondrial and
1792 ER-derived pre-peroxisomes. *Nature* 542:251-4.
- 1793 Simson P, Jephthina N, Laasmaa M, Peterson P, Birkedal R, Vendelin M (2016) Restricted ADP movement in
1794 cardiomyocytes: Cytosolic diffusion obstacles are complemented with a small number of open mitochondrial
1795 voltage-dependent anion channels. *J Mol Cell Cardiol* 97:197-203.
- 1796 Stucki JW, Ineichen EA (1974) Energy dissipation by calcium recycling and the efficiency of calcium transport
1797 in rat-liver mitochondria. *Eur J Biochem* 48:365-75.
- 1798 Tonkonogi M, Harris B, Sahlin K (1997) Increased activity of citrate synthase in human skeletal muscle after a
1799 single bout of prolonged exercise. *Acta Physiol Scand* 161:435-6.
- 1800 Torralba D, Baixauli F, Sánchez-Madrid F (2016) Mitochondria know no boundaries: mechanisms and functions
1801 of intercellular mitochondrial transfer. *Front Cell Dev Biol* 4:107. eCollection 2016.
- 1802 Vamecq J, Schepers L, Parmentier G, Mannaerts GP (1987) Inhibition of peroxisomal fatty acyl-CoA oxidase by
1803 antimycin A. *Biochem J* 248:603-7.
- 1804 Waczulikova I, Habodaszova D, Cagalinec M, Ferko M, Ulicna O, Mateasik A, Sikurova L, Ziegelhöffer A
1805 (2007) Mitochondrial membrane fluidity, potential, and calcium transients in the myocardium from acute
1806 diabetic rats. *Can J Physiol Pharmacol* 85:372-81.
- 1807 Wagner BA, Venkataraman S, Buettner GR (2011) The rate of oxygen utilization by cells. *Free Radic Biol Med*
1808 51:700-712.
- 1809 Wang H, Hiatt WR, Barstow TJ, Brass EP (1999) Relationships between muscle mitochondrial DNA content,
1810 mitochondrial enzyme activity and oxidative capacity in man: alterations with disease. *Eur J Appl Physiol*
1811 *Occup Physiol* 80:22-7.
- 1812 Watt IN, Montgomery MG, Runswick MJ, Leslie AG, Walker JE (2010) Bioenergetic cost of making an
1813 adenosine triphosphate molecule in animal mitochondria. *Proc Natl Acad Sci U S A* 107:16823-7.
- 1814 Weibel ER, Hoppeler H (2005) Exercise-induced maximal metabolic rate scales with muscle aerobic capacity. *J*
1815 *Exp Biol* 208:1635–44.
- 1816 White DJ, Wolff JN, Pierson M, Gemmell NJ (2008) Revealing the hidden complexities of mtDNA inheritance.
1817 *Mol Ecol* 17:4925–42.

- 1818 Wikström M, Hummer G (2012) Stoichiometry of proton translocation by respiratory complex I and its
 1819 mechanistic implications. *Proc Natl Acad Sci U S A* 109:4431-6.
 1820 Williams EG, Wu Y, Jha P, Dubuis S, Blattmann P, Argmann CA, Houten SM, Amariuta T, Wolski W,
 1821 Zamboni N, Aebersold R, Auwerx J (2016) Systems proteomics of liver mitochondria function. *Science* 352
 1822 (6291):aad0189
 1823 Willis WT, Jackman MR, Messer JI, Kuzmiak-Glancy S, Glancy B (2016) A simple hydraulic analog model of
 1824 oxidative phosphorylation. *Med Sci Sports Exerc* 48:990-1000.
 1825 Zíková A, Hampl V, Paris Z, Týč J, Lukeš J (2016) Aerobic mitochondria of parasitic protists: diverse genomes
 1826 and complex functions. *Mol Biochem Parasitol* 209:46-57.
 1827
 1828

1829 Supplement

1830 S1. Manuscript phases and versions - an open-access approach

1831 This manuscript on ‘Mitochondrial respiratory states and rates’ is a position statement in the frame of COST Action
 1832 CA15203 MitoEAGLE. The global MitoEAGLE network made it possible to collaborate with a large number of
 1833 co-authors to reach consensus on the present manuscript. Nevertheless, we do not consider scientific progress to
 1834 be supported by ‘declaration’ statements (other than on ethical or political issues). Our manuscript aims at
 1835 providing arguments for further debate rather than pushing opinions. We hope to initiate a much broader process
 1836 of discussion and want to raise the awareness of the importance of a consistent terminology for reporting of
 1837 scientific data in the field of bioenergetics, mitochondrial physiology and pathology. Quality of research requires
 1838 quality of communication. Some established researchers in the field may not want to re-consider the use of jargon
 1839 which has become established despite deficiencies of accuracy and meaning. In the long run, superior standards
 1840 will become accepted. We hope to contribute to this evolutionary process, with an emphasis on harmonization
 1841 rather than standardization.
 1842

1843 *Phase 1* The protonmotive force and respiratory control

1844 http://www.mitoeagle.org/index.php/The_protonmotive_force_and_respiratory_control

- 1845 • 2017-04-09 to 2017-09-18 (44 versions)
- 1846 • 2017-09-21 to 2018-02-06 (44+21 versions)

1847 http://www.mitoeagle.org/index.php/MitoEAGLE_preprint_2017-09-21

1848 2017-11-11: Print version (16) for MiP2017/MitoEAGLE conference in Hradec Kralove

1849 *Phase 2* Mitochondrial respiratory states and rates: Building blocks of mitochondrial physiology Part 1

1850 http://www.mitoeagle.org/index.php/MitoEAGLE_preprint_2018-02-08

- 1851 • 2018-02-08 – (44+48 Versions up to 2018-11-28)

1852 *Phase 3* Mitochondrial respiratory states and rates. Submission to a preprint server: [BioRxiv](https://www.biorxiv.org/)

1853 *Phase 4* Journal submission: CELL METABOLISM, aiming at indexing by *The Web of Science* and *PubMed*.
 1854
 1855

1856 S2. Authors

1857 This manuscript developed as an open invitation to scientists and students to join as co-authors in the bottom-up
 1858 spirit of COST, to provide a balanced view of mitochondrial respiratory control and a consensus statement on
 1859 reporting data of mitochondrial respiration in terms of metabolic flows and fluxes.

1860 Co-authors are added in alphabetical order based upon a first draft written by the corresponding author,
 1861 who edited all versions. *Co-authors confirm that they have read the final manuscript, possibly have made additions
 1862 or suggestions for improvement, and agree to implement the recommendations into future manuscripts,
 1863 presentations and teaching materials.*

1864 We continue to invite comments and suggestions, particularly if you are an early career investigator adding
 1865 an open future-oriented perspective, or an established scientist providing a balanced historical basis. Your critical
 1866 input into the quality of the manuscript will be most welcome, improving our aims to be educational, general,
 1867 consensus-oriented, and in practice be helpful to students working in mitochondrial respiratory physiology.

1868 To join as a co-author, please feel free to focus on a particular section, providing direct input and references,
 1869 and contributing to the scope of the manuscript from the perspective of your expertise. Your comments will be
 1870 considered as appropriate in the manuscript and will be largely posted on the discussion page of the MitoEAGLE
 1871 preprint website.
 1872
 1873

1874 S3. Joining COST Actions

- 1875 • CA15203 MitoEAGLE - http://www.cost.eu/COST_Actions/ca/CA15203
- 1876 • CA16225 EU-CARDIOPROTECTION - http://www.cost.eu/COST_Actions/ca/CA16225
- 1877 • CA17129 CardioRNA - http://www.cost.eu/COST_Actions/ca/CA17129



Mitochondrial respiratory states and rates:



Building blocks of mitochondrial physiology

Part 1 - www.mitoeagle.org/index.php/MitoEAGLE_preprint_2018-02-08

Gnaiger E^{1,2}, corresponding author
355 co-authors, MitoEAGLE Working Group

¹Medical University Innsbruck
²Oroboros, Innsbruck, Austria

Aims Clarity of concept and consistency of nomenclature facilitate effective transdisciplinary communication, education, and ultimately further discovery.

Adhering to uniform standards and harmonizing the terminology concerning mitochondrial respiratory states and rates will support the development of databases of mitochondrial respiratory function in cells, tissues, and species.

Summary Recommendations on coupling control states and rates are focused on studies with mitochondrial preparations.

Fig. 1: Respiration is defined by O₂ flux balance.
Fig. 2: OXPHOS analysis is based on the study of mt- preparations. Metabolic fluxes measured in defined coupling and pathway control states provide insights into the meaning of cellular respiration.
Fig. 3: Interpretation of respiratory rates depends critically on appropriate normalization.

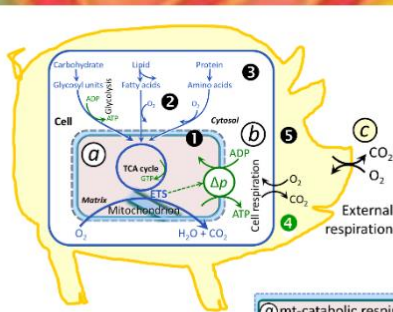
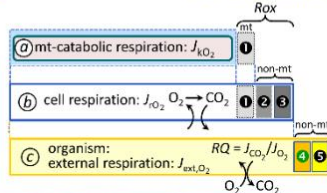


Figure 1. From mitochondrial to external respiration

Mitochondrial (mt) respiration is the oxidation of fuel substrates (electron donors) and reduction of O₂ catalysed by the electron transfer system, ETS:

- a** mt-catabolic respiration, excluding
- 1** mt-residual oxygen consumption, *Rox*.
- b** Total cellular O₂ consumption, including mt-*Rox*, **e** non-mt catabolic *Rox*, particularly by peroxisomal oxidases, and **e** non-mt *Rox* unrelated to catabolism.
- c** External respiration, including **1** aerobic microbial respiration, and **e** extracellular O₂ consumption.



MIPart by Odra Noel

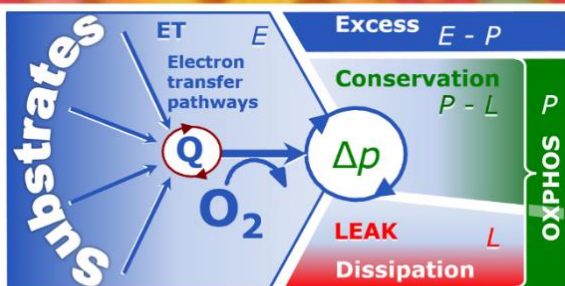


Figure 2. Respiratory states (ET, OXPHOS, LEAK) and corresponding rates (E, P, L)

Table 1. Coupling states and residual oxygen consumption in mitochondrial preparations in relation to respiration- and phosphorylation-flux, J_{kO_2} and J_{p_0} , and protonmotive force, Δp . Coupling states are established at kinetically-saturating concentrations of fuel substrates and O₂.

State	J_{kO_2}	J_{p_0}	Δp	Inducing factors	Limiting factors
LEAK	L ; low, cation leak-dependent respiration	0	max.	proton leak, slip, and cation cycling	$J_{p_0} = 0$: (1) without ADP, L_{sc} ; (2) max. ATP/ADP ratio, L_r ; or (3) inhibition of the phosphorylation-pathway, L_{Oxy}
OXPHOS	P ; high, ADP-stimulated respiration	max.	high	kinetically-saturating [ADP] and [P _i]	J_{p_0} , by phosphorylation-pathway; or J_{kO_2} by ET-capacity
ET	E ; max., noncoupled respiration	0	low	optimal external uncoupler concentration for max. $J_{O_{2,E}}$	J_{kO_2} by ET-capacity
ROX	Rox ; min., residual O ₂ consumption	0	0	$J_{O_{2,Rox}}$ in non-ET-pathway oxidation reactions	inhibition of all ET-pathways; or absence of fuel substrates

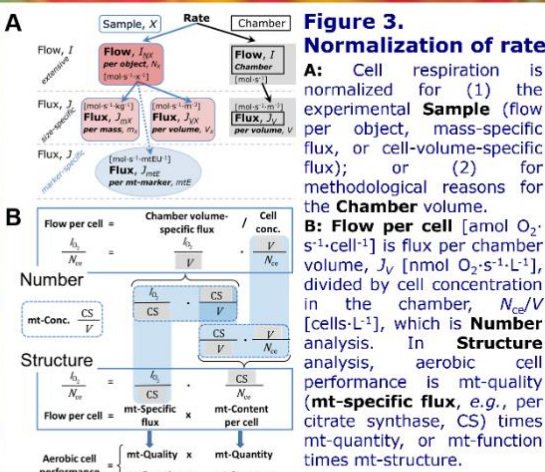


Figure 3. Normalization of rate

A: Cell respiration is normalized for (1) the experimental **Sample** (flow per object, mass-specific flux, or cell-volume-specific flux); or (2) for methodological reasons for the **Chamber** volume.
B: **Flow per cell** [amol O₂ s⁻¹ cell⁻¹] is flux per chamber volume, J_V [nmol O₂ s⁻¹ L⁻¹], divided by cell concentration in the chamber, N_{ce}/V [cells L⁻¹], which is **Number** analysis. In **Structure** analysis, aerobic cell performance is mt-quality (**mt-specific flux**, e.g., per citrate synthase, CS) times mt-quantity, or mt-function times mt-structure.

cost
EUROPEAN COOPERATION IN SCIENCE & TECHNOLOGY
Funded by the Horizon 2020 Framework Programme of the European Union

MitoEAGLE
Join
COST Action CA15203
www.mitoeagle.org/index.php/MitoEAGLE

COST Action CA15203 MitoEAGLE

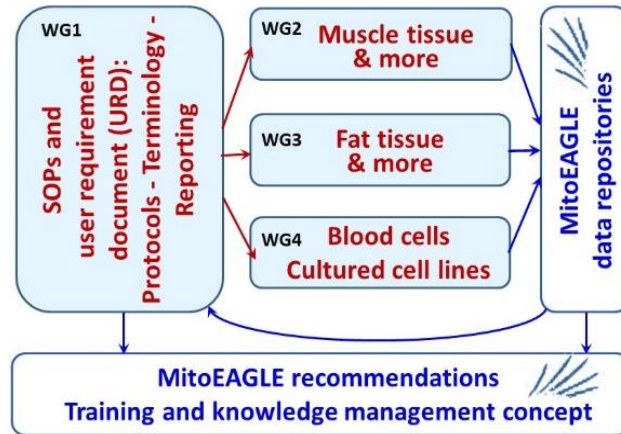
Evolution Age Gender
Lifestyle Environment



Mission of the global MitoEAGLE network

in collaboration with the Mitochondrial Physiology Society, MiPs

- Improve our knowledge on mitochondrial function in health and disease with regard to Evolution, Age, Gender, Lifestyle and Environment
- Interrelate studies across laboratories with the help of a MitoEAGLE data management system
- Provide standardized measures to link mitochondrial and physiological performance to understand the myriad of factors that play a role in mitochondrial physiology



Join the COST Action MitoEAGLE - contribute to the quality management network.



More information:
www.mitoeagle.org



Funded by the Horizon 2020 Framework Programme
of the European Union

